Mathematisches Forschungsinstitut Oberwolfach

Report No. 42/2022

DOI: 10.4171/OWR/2022/42

Multiscale Wave-Turbulence Dynamics in the Atmosphere and Ocean

Organized by
Ulrich Achatz, Frankfurt
Oliver Bühler, New York
Chantal Staquet, Grenoble
William Young, La Jolla

18 September – 24 September 2022

Abstract. The atmosphere and oceans present an ongoing first-rate challenge to science and mathematics because they operate on an extremely broad ranges of scales, from molecular to planetary in length and from below seconds to millennia in time. This is the reason why climate simulations still suffer from leading-order uncertainties. Conceptual simplifications, such as scale-separation assumptions and the neglect of many physical processes, have enabled past progress in understanding the interactions of the basic dynamic constituents, i.e. large-scale mean flows, medium-scale waves and vortices, and small-scale turbulence. But present-day research is stretching the validity of this framework. For example, it is recognized that intermediate-scale waves and vortices are key elements linking all relevant players, and are often characterized by nonlinear interactions on comparable scales and also by additional physical nonlinearities due to effects such as air moisture. Motivated by recent advances in mathematical wave–vortex and wave–wave interaction theory, turbulence theory, and the study of internal wave dynamics as well as their numerical parametrization, the workshop gathered leading experts in these fields to foster a synthesis of new approaches and thereby a new level of understanding and numerical treatment of climate dynamics.

Mathematics Subject Classification (2020): 76-XX, 76Uxx.

Introduction by the Organizers

Our workshop *Multiscale Wave-Turbulence Dynamics in the Atmosphere and Ocean* was very well attended and enthusiastically received by in-person participants from all corners of the world, including participants from Australia and India. Some scientists could only attend online, and we are grateful that the broadcasting system for the talks worked very well for these remote participants.

The spectrum of attendees was exceptionally broad, ranging from mathematicians and numerical analysts to oceanographers, meteorologists, turbulence experts, and climate scientists. Common to all was the desire to foster a strong interdisciplinary dialogue and to initiate or deepen collaborations across the narrow confines of traditional scientific disciplines. We feel that in that our workshop exceeded our expectations, a sentiment that was echoed to us by many of the participants.

The workshop itself followed the usual routine of week-long workshops at the MFO, with the exception that on Monday afternoon we held a poster session, which served very well as a starting point for discussions and also as an icebreaker for the participants, for whom this was the first in-person workshop since Covid in many cases. We think such a poster session is very valuable and would recommend that to other workshop organizers, not least because traditionally there are significantly fewer talks than participants at MFO workshops.

The remainder of this report contains in alphabetical order the abstracts of the twenty-one oral presentations given at the workshop, which illustrate the high quality and the wide topical range of the science presented at our meeting. Finally, we are very grateful for the exceptional support and professionalism of the many heads and hands at MFO that made our workshop such a pleasant and stimulating reality.

For the organizers: Oliver Bühler, New York, October 2022.

Workshop: Multiscale Wave-Turbulence Dynamics in the Atmosphere and Ocean

Table of Contents

T. R. Akylas (joint with Boyu Fan, Christos Kakoutas)
Short-scale Instabilities of Internal Gravity Waves: From Floquet Analysis to PSI and Beyond 2471

Roy Barkan (joint with Roy Barkan, Kaushik Srinivasan, Luwei Yang, Subhajit Kar, Michal Shaham, James C. McWilliams)
Eddy-wave interactions and turbulent cascades in oceanic numerical simulations of varying complexity 2472

Jörn Callies (joint with Henry G. Peterson)
Coupling between bottom boundary layers and the large-scale circulation of the abyssal ocean 2475

Colin Cotter (joint with Werner Bauer, Beth Wingate, Hiroe Yamazaki)
Numerical phase averaging for geophysical fluid dynamics 2477

Stamen I. Dolaptchiev (joint with Peter Spichtinger, Manuel Baumgartner, Ulrich Achatz)
Asymptotic modeling of ice nucleation due to gravity waves 2479

Nicolas Grisouard (joint with Fabiloa Trujano-Jiménez, Varvara E. Zemskova)
Ekman-inertial instability 2481

Pedram Hassanzadeh
Learning Data-driven Subgrid-Scale Models for Geophysical Turbulence: Stability, Extrapolation & Interpretation 2482

Hossein Kafiabad (joint with Jacques Vanneste)
Computing Lagrangian means without tracking particles 2484

Francois Lott
Parameterization of non-orographic gravity waves in large-scale models. Formalism, impact and test against direct observations. 2485

Leo Maas
Inertial wave attractor induced mean flow and vortex cluster 2486

Callum Shakespeare (joint with Brian K. Arbic, Andy McC. Hogg)
New perspectives on the wave drag and pseudo-momentum flux of the oceanic internal tide 2487

Victor I. Shrira (joint with Sergei I. Badulin, Rema Almelah)
How does wave field evolution drive surface ocean currents? 2488

Joel Sommeria (joint with Hamed Vaziri, Antoine Venaille)
Modelling vertical mixing by statistical mechanics at a density interface 2490

Ivana Stiperski (joint with Marc Calaf)
Monin-Obukhov Similarity Theory and its Generalization for Complex Atmospheric Turbulence 2492

Bruce R. Sutherland
The Nonlinear Evolution of Internal Tides 2494

Jim Thomas
Turbulent dynamics of the balanced flow in the ocean 2495

Jacques Vanneste (joint with M. R. Cox, M. A. C. Savva, H. A. Kafiabad)
Scattering of inertia-gravity waves by geostrophic flows 2496

Nikki Vercauteren (joint with Vyacheslav Boyko, Sebastian Krumscheid)
Uncertain turbulent fluxes in the atmospheric boundary layer: a stochastic data-model fusion approach 2497

Georg S. Voelker (joint with Young-Ha Kim, Gergely Bölöni, Günther Zängl, Ulrich Achatz)
MS-GWaM – A three dimensional transient parametrization for internal gravity waves in atmospheric models 2499

Gregory L. Wagner (joint with Nick Pizzo, Luc Lenain, Fabrice Veron)
Instability and turbulent mixing in wind-driven shear layers 2502

Han Wang (joint with Nicolas Grisouard, Hesam Salehipour, Alice Nuz, Michael Poon, Aurélien L. Ponte, Brian Arbic)
A deep learning approach to extract surface internal tidal signals scattered by geostrophic turbulence 2504

Abstracts

Short-scale Instabilities of Internal Gravity Waves: From Floquet Analysis to PSI and Beyond

T. R. Akylas

(joint work with Boyu Fan, Christos Kakoutas)

The stability of internal gravity waves in a continuously stratified fluid is a problem of fundamental and geophysical interest. Early work focused on sinusoidal plane waves in an inviscid Boussinesq fluid with constant buoyancy frequency. In this idealized setting, linear stability analysis based on Floquet theory has revealed a wide host of instabilities with varying dynamics and physical mechanisms (e.g. see Sonmor & Klaassen [1] and Yau, Klaassen & Sonmor [2] for a comprehensive treatment). As first noted by Mied [3], in the limit of small primary-wave amplitude, this diverse range of instabilities reduce to triad resonance interactions: the primary wave is unstable to two sinusoidal subharmonic perturbations whose frequencies and wavevectors sum to those of the basic state. A specific form of such triadic resonance instability (TRI), where the subharmonic perturbations have half the frequency of the primary wave and very fine wavelength, is the celebrated parametric subharmonic instability (PSI). This mechanism has attracted considerable interest as it permits transfer of energy into much smaller scales (e.g. Staquet & Sommeria [4]) and therefore may be a potentially significant factor in the dissipation of oceanic internal waves (Hibiya, Nagasawa & Niwa [5]; MacKinnon & Winters [6]; Young, Tsang & Balmforth [7]).

The present work is an effort to understand instability mechanisms of more general internal gravity wave disturbances than sinusoidal plane waves. Specifically, attention is focused on short-scale instabilities of finite-width wave beams in an unbounded fluid and on wave modes in a waveguide, such as the ocean thermocline. These types of wave disturbances arise in oceans due to the interaction of the barotropic tide with bottom topography (Lamb [8]; Cole *et al.* [9]; Johnston *et al.* [10]) and therefore provide a more realistic setting for instability. However, compared with sinusoidal waves, formal stability analysis based on Floquet theory is more demanding, as it requires solving an eigenvalue problem that involves an infinite number of differential, rather than algebraic, equations.

Here, the Floquet stability eigenvalue problem that pertains to wave beams and wave modes is studied asymptotically in the limit where PSI becomes relevant, namely for a small-amplitude ($\epsilon \ll 1$) basic state subject to fine-scale (dimensionless wavenumber $k \gg 1$) perturbations under nearly inviscid conditions ($\nu = 1/Re \ll 1$). It is argued that the nature of instability in this regime hinges on the magnitude of ϵk: PSI, where two short-scale perturbations at half the basic-wave frequency interact resonantly with the basic wave, is appropriate only when $\epsilon k = O(\sqrt{\epsilon})$ or smaller; for shorter perturbations, $\epsilon k = O(1)$, higher frequency components come into play due to the advection of the perturbation by the underlying wave, resulting in broadband instability. This novel, essentially inviscid

($\nu = O(\epsilon^3)$) mechanism can cause instability of finite-width beams that are not generally susceptible to PSI (Fan & Akylas [11]), but also may suppress PSI of internal wave modes (Akylas & Kakoutas [12]).

References

[1] Sonmor, L.J. & Klaassen, G.P. *Toward a unified theory of gravity wave stability* J. Atmos. Sci. **54** (22) (1997), 2655–2680.

[2] Yau, K.H., Klaassen, G.P. & Sonmor, L.J. *Principal instabilities of large amplitude inertio-gravity waves* Phys. Fluids **16** (4) (2004), 936–951.

[3] Mied, R.P. *The occurrence of parametric instabilities in finite-amplitude internal gravity waves* J. Fluid Mech. **78** (4) (1976), 763–784.

[4] Staquet, C. & Sommeria, J. *Internal gravity waves: from instabilities to turbulence* Annu. Rev. Fluid Mech. **34** (1) (2002), 559–593.

[5] Hibiya, T., Nagasawa, M. & Niwa, Y. *Nonlinear energy transfer within the oceanic internal wave spectrum at mid and high latitudes* J. Geophys. Res. **107** (C11)(2002), 3207.

[6] Mackinnon, J.A. & Winters, K.B. *Subtropical catastrophe: significant loss of low-mode tidal energy at 28.9°* Geophys. Res. Lett. **32** (15) (2005), L15605.

[7] Young, W.R., Tsang, Y.-K. & Balmforth, N.J. *Near-inertial parametric subharmonic instability* J. Fluid Mech. **607** (2008), 25–49.

[8] Lamb, K.G. *Nonlinear interaction among internal wave beams generated by tidal flow over supercritical topography* Geophys. Res. Lett. **31** (9) (2004), L09313.

[9] Cole, S.T., Rudnick, D.L., Hodges, B.A. & Martin, J.P. *Observations of tidal internal wave beams at Kauai Channel, Hawaii* J. Phys. Oceanogr. **39** (2) (2009), 421–436.

[10] Johnston, T.M.S., Rudnick, D.L., Carter, G.S., Todd, R.E. & Cole, S.T. *Internal tidal beams and mixing near monterey bay* J. Geophys. Res. **116** (2011), C03017.

[11] Fan, B. & Akylas, T.R. *Finite-amplitude instabilities of thin internal wave beams: experiments and Theory* J. Fluid Mech. **904**, (2020) A16.

[12] T.R. Akylas & C. Kakoutas, *Stability of internal gravity wave modes: from triad resonance to broadband instability*, J. Fluid Mech (2022), submitted.

Eddy-wave interactions and turbulent cascades in oceanic numerical simulations of varying complexity

Roy Barkan

(joint work with Roy Barkan, Kaushik Srinivasan, Luwei Yang, Subhajit Kar, Michal Shaham, James C. McWilliams)

The general circulation of the ocean is forced by boundary fluxes of momentum, heat, and freshwater at basin scales. These spatially and temporally variable boundary forces provide energy sources that drive a circulation with flow features that vary on a wide range of spatial and temporal scales. Climate equilibrium can only be reached through dissipation of these energy sources, which in the ocean occurs at centimeter scales. Mesoscale eddies are well known as the dominant reservoir of kinetic energy (KE) in the oceans ([1]), but because their dynamics are constrained by an approximate geostrophic and hydrostatic force balance they are characterized by an inverse KE cascade, and by themselves do not provide the necessary forward scale-transfer to dissipation. Possible mechanisms for the KE route to dissipation (often referred to as loss-of-balance) include interaction with the bottom boundary layer ([2, 3]) and instabilities that are strongly linked to

the formation of submesoscale currents (SMCs; [4]). In contrast with mesoscale eddies, which have time scales of weeks to months and are characterized by Rossby number $Ro \ll 1$, SMCs, comprising fronts, filaments, and mixed-layer eddies, are much more rapidly evoloving (time scales of about a day) and non-linear, and are therefore characterized by $Ro \sim \mathcal{O}(1)$.

Oceanic internal waves (IWs) are fast motions with intrinsic frequencies ω in the range $f < \omega < N$, where f and N are the (local) Coriolis and Brunt Väisälä frequencies, respectively. They are predominantly forced by atmospheric storms, which generate IWs with $\omega \sim f$ (e.g., near-inertial waves; NIWs), and by the barotropic tide flowing over topography, which generates internal-waves dominated by $\omega \sim M_2$, where M_2 is the semidiurnal tidal frequency (e.g., semidiurnal internal tides). Despite this narrow-band IW forcing, observations show that oceanic IWs have a broadband energy distribution that follows the so-called Garrett-Munk ([5]) continuum spectrum.

Recently, [6] and [7] developed an asymptotic theory that shows that NIWs can extract energy from quasigeostrophic flow (i.e., $Ro \ll 1$). Furthermore, [8] and [9] suggested that a steady quasigeostrophic flow can spectrally diffuse IW energy in the wavenumber direction and [10] demonstrated that if the quasigeostrophic flow is allowed to be slowly varying then diffusion in the frequency direction is also possible.

In this work we aim to bridge the gap between the theoretical predictions and realistic numerical solutions and investigate whether interactions between (sub)mesoscale eddies and IWs can lead to loss-of-balance and to the depletion of oceanic mesoscale eddies, and whether the refraction and scattering of IWs by (sub)mesoscale eddies contribute to the 'filling' up of the continuum spectrum. We extend previous work by exploring the interactions in a dynamical regime with $Ro \sim \mathcal{O}(1)$, which is prevalent in the oceanic mixed layer during winter.

Our methodology relies on quantifying cross-scale transfers of KE in a multitude of numerical solutions ranging from idealized 2D 'toy' models, to state-of-the-art realistically forced ocean simulations. To this end we adopt the Gallilean-invriant Coarse-graining framework of [11] and decompose the velocity fields into scales smaller (faster) and larger (slower) than a given length scale ℓ (time scale τ) with a low-pass filtering function such that $u_i = \overline{u}^{\ell} + u'^{\ell}$, or $u_i = \overline{u}^{\tau} + u'^{\tau}$, where $i \in [1, 2]$ and $(u_1, u_2) = (u, v)$. The associated energy transfer is then

$$\Pi = \underbrace{-(\tau_{uu}\overline{u}_x + \tau_{uv}(\overline{u}_y + \overline{v}_x) + \tau_{vv}\overline{v}_y)}_{\Pi_h} \underbrace{-(\tau_{uw}\overline{u}_z + \tau_{vw}\overline{v}_z)}_{\Pi_v}, \tag{1}$$

where the bar operator denotes either spatial or temporal filters and Π_h and Π_v are the horizontal and vertical energy transfer terms. The Leonard stress term ([12]) is $\tau_{uv} = \overline{uv} - \overline{u}\,\overline{v}$, and similarly for the other terms. The horizontal energy transfer term can also be written as ([13])

$$\Pi_h = \underbrace{\frac{(\tau_{vv} - \tau_{uu})}{2}\overline{\sigma}_n - \tau_{uv}\overline{\sigma}_s}_{\Pi_\alpha} \underbrace{-\frac{(\tau_{vv} + \tau_{uu})}{2}\overline{\delta}}_{-\Pi_\delta}, \tag{2}$$

where $\overline{\sigma}_n$, $\overline{\sigma}_s$, and $\overline{\delta}$ are the normal strain, shear strain, and horizontal divergence of the filtered fields, respectively. Π_α is sometime referred to as the deformation shear production ([14]) and in [13] we call $\Pi_\delta = -\overline{\delta}\mathcal{E}'$ the convergence production, with $\mathcal{E}'$ denoting the KE of the smaller scale (high-passed) fields. The form of Π_δ illustrates that a forward energy cascade is expected to take place in convergent regions. Such convergent regions in the ocean are typically found at submesoscale fronts and filaments, where a substantial departure from geostrophic balance is at play due to the prominent ageostrophic secondary circulation. Using idealized 2D simulations of vertical IW modes in a semigeostrophic ([15]) frontal zone, we demonstrated that the convergence-production is an efficient mechanism allowing IWs to extract KE from the frontal circulation. Accordingly, we found that the strongest forward temporal KE cascade in realistically-forced numerical solutions with both (sub)mesoscale eddies and IWs was in surface-intensified convergent fronts and filaments ([16]). Furthermore, the realistic solutions with IW forcing exhibited a reduction in the inverse cascade compared with solutions where IWs were absent. These IW-induced modified turbulent cascades resulted in a substantial depletion of mesoscale KE.

To study eddy-effects on IW frequency spreading we examined the gradual development of the continuum frequency spectra in waveless solutions forced by an inertially-resonant atmospheric storm. Comparing solutions with and without a background eddy field we showed that refraction by (sub)mesoscale eddies is crucial to filling up the spectral gaps between the inertial peak and the associated superharmonics. By comparing Eulerian-based and Lagrangian-based spectral estimates we further determined that Doppler-shifting played a negligible role in the region of study.

To explore IW-scattering, we decompose the velocity field u_i into 'eddy' and 'IW' components u_i^e and u_i^w, using temporal low-passed filtering and a Helmholtz decomposition, and examined the associated spatial cross-scale energy transfers. Plugging this eddy-wave decomposition into Eq. (1), the Leonard stress terms become, e.g., $\tau_{uv} = \tau_{uv}^{ee} + \tau_{uv}^{ew} + \tau_{uv}^{we} + \tau_{uv}^{ww}$, and the associated coarse-grained fluxes are

$$\Pi = \Pi^{Www} + \Pi^{Eee} + \Pi^{Eww} + \Pi^{Wee} + \Pi^{Eew} + \Pi^{Ewe} + \Pi^{Wew} + \Pi^{Wwe}. \tag{3}$$

In Eq. (3), lowercase letters denote the smaller scale (Leonard) stress-terms and the uppercase letters denote the spatially low-passed strain, divergence, and vertical shear terms. In particular, scattering is quantified by $\Pi^{Wew} + \Pi^{Wwe}$, and can be compared with Π^{Www}, which quantifies wave-wave interactions. Interestingly, we found that scattering was the dominant term leading to the forward KE cascade, especially in Π_v, supporting the findings of the earlier theories.

References

[1] Wunsch, C and R. Ferrari, "Vertical Mixing, Energy, and the General Circulation of the Oceans", *Ann. Rev. Fluid Mech.*, 2004, vol. 36, pp. 281-314.

[2] McWilliams, James C. "Submesoscale currents in the ocean." Proceedings of the Royal Society A: Mathematical, Physical and Engineering Sciences 472.2189 (2016): 20160117.

[3] Nikurashin, M. and Vallis, G. K. and Adcroft, A. "Routes to energy dissipation for geostrophic flows in the Southern Ocean",*Nature Geoscience*, 2013, vol. 6, pp. 48-51.
[4] Capet, X and J. C. McWilliams and M. J. Molemaker and A. F. Shchepetkin. "Mesoscale to submesoscale transition in the California Current System. Part I: Flow Structure, Eddy Flux, and Observational Tests", *J. Phys. Ocean.*, 2008, vol. 38, pp. 29-43.
[5] C. J. R. Garrett and W. H. Munk. "Space-time scales of internal waves." *Geophys. Fluid Dynamics.*, 1972, pp. 225-264.
[6] Xie, J-H., and Jacques Vanneste. "A generalised-Lagrangian-mean model of the interactions between near-inertial waves and mean flow." *Journal of Fluid Mechanics*, 2015, vol. 774, pp. 143-169.
[7] Wagner, G. L., and W. R. Young. "A three-component model for the coupled evolution of near-inertial waves, quasi-geostrophic flow and the near-inertial second harmonic." *Journal of Fluid Mechanics*, 2016, vol. 802, pp. 806-837.
[8] Kafiabad, Hossein A., Miles AC Savva, and Jacques Vanneste. "Diffusion of inertia-gravity waves by geostrophic turbulence." *Journal of Fluid Mechanics*, 2019, vol. 869.
[9] Savva M. A. C. & Vanneste J. "Scattering of internal tides by barotropic quasigeostrophic flows". *J. Fluid Mech.*, 2018, vol. 856, pp. 504-530.
[10] Dong, Wenjing, Oliver Bühler, and K. Shafer Smith. "Frequency diffusion of waves by unsteady flows". *Journal of Fluid Mechanics*, 2020, vol. 905.
[11] Eyink, Gregory L., and Hussein Aluie. "Localness of energy cascade in hydrodynamic turbulence. I. Smooth coarse graining." *Physics of Fluids*, 2009, vol. 21, pp. 107-115.
[12] Leonard, A. "Energy cascade in large-eddy simulations of turbulent fluid flows". *Advances in Geophysics A*, 1974, vol. 18, pp. 237-248.
[13] Srinivasan, Kaushik, Roy Barkan, and James C. McWilliams. "A forward energy flux at submesoscales driven by frontogenesis." *Journal of Physical Oceanography*, 2022, accepted.
[14] Thomas, Leif N. "On the effects of frontogenetic strain on symmetric instability and inertiaÐgravity waves." *Journal of Fluid Mechanics*, 2012, vol. 711, pp. 620-640.
[15] Hoskins, J. H and Bretherton, F.P. "Atmospheric frontogenesis models: Mathematical formulation and solution". *J. atmos. Sci.*, 1972, vol. 29, pp.1-37.
[16] Barkan, R., Srinivasan, K., Yang, L., McWilliams, J. C., Gula, J., and Vic, C. "Oceanic mesoscale eddy depletion catalyzed by internal waves." *Geophys. Res. Letts*, 2001, vol. 48(18), pp. e2021GL094376.

Coupling between bottom boundary layers and the large-scale circulation of the abyssal ocean

Jörn Callies
(joint work with Henry G. Peterson)

A long-standing question in oceanography is how internal waves–and the small-scale turbulence they produce when breaking–interact with the mean overturning circulation of the abyssal ocean. Small-scale turbulence is required to lighten dense bottom waters formed around Antarctica, allowing these waters to upwell across density surfaces to mid-depths and close the overturning loop. Observational work over the past few decades has revealed that vigorous turbulence is confined to regions where tidal or geostrophic flows pass over a rough seafloor. Such turbulence over rough topography is strongest in the bottom few hundred meters and weakens substantially above, a vertical structure which implies that interior waters in fact gain density. It is only in a thin bottom boundary layer that water parcels become

lighter and upwell along the sloping seafloor, meaning these boundary layers should take center stage in any theory of the abyssal overturning circulation [1, 2].

Here, we aim to understand both how the flow locally responds to bottom-intensified mixing on slopes and how the local responses in different locations combine to a global circulation. We apply boundary layer theory to the planetary geostrophic equations to capture the two-way interaction between the boundary layer and the interior. This analysis reveals that the boundary layer feeds back on the interior both by balancing turbulent buoyancy fluxes with cross-slope advection and by producing convergent or divergent boundary layer mass transport that injects fluid into the interior or sucks fluid out of the interior, similar to how wind forcing produces Ekman pumping and suction in the upper ocean. We argue that these boundary layer–interior interactions are at the core of the mixing-driven circulation of the abyssal ocean.

Specifically, we revise the one-dimensional model traditionally employed to understand the response of a rotating and stratified fluid to mixing over a sloping seafloor [3, 4, 5, 6, 7]. We point out that such a one-dimensional model captures the evolution on the flank of a two-dimensional ridge only if a constraint is imposed on the vertically integrated cross-slope transport. A transport constraint can be imposed if the model also allows for a barotropic (vertically uniform) cross-slope pressure gradient. We demonstrate the success of this revised model, and we apply boundary layer theory to gain insight into its dynamics. This reveals that the cross-slope boundary layer transport is $\mu S/(1+\mu S)\,\kappa\cot\theta$, where $\mu = \nu/\kappa$ is the turbulent Prandtl number, $S = N^2\tan^2\theta/f^2$ is the slope Burger number, and θ is the slope angle of the seafloor with respect to the horizontal. The turbulent mixing coefficients κ and ν are evaluated at the top of the boundary layer. The cross-slope buoyancy advection by this boundary layer transport balances buoyancy diffusion into the boundary layer, thus providing an effective boundary condition on the interior evolution that takes this boundary layer process into account. In two dimensions, variations in the boundary layer transport can furthermore affect the interior evolution through mass fluxes that must be absorbed or supplied by the interior. Importantly, the above expression for the boundary layer transport is globally valid, unlike a similar expression emerging in the traditional one-dimensional model.

So far, we have only considered one- and two-dimensional dynamics [8, 9]. Currently, we are extending our approach to three dimensions, where new phenomenology awaits. In one and two dimensions, the along-slope momentum balance always involves friction, even outside of the boundary layer, because the symmetry precludes pressure gradients in this direction. In three dimensions, in contrast, the interior momentum balance can be fully geostrophic. Furthermore, buoyancy advection by the geostrophic flow is trivial in one and two dimensions because the geostrophic flow is directed along the slope, where there are no buoyancy gradients. The buoyancy evolution is thus slow, governed by ageostrophic cross-slope advection and vertical diffusion. This changes in three dimensions because the geostrophic flow can now act on non-zero buoyancy gradients, producing a fast

evolution. We expect that boundary layer theory will again allow for deep insight into these dynamics and elucidate the workings of the abyssal circulation of the real ocean.

References

[1] R. Ferrari, A. Mashayek, T. J. McDougall, M. Nikurashin, J.-M. Campin, *Turning Ocean Mixing Upside Down*, Journal of Physical Oceanography **46** (2016), 2239–2261.

[2] C. de Lavergne, G. Madec, J. Le Sommer, A. J. G. Nurser, A. C. Naveira Garabato, *On the Consumption of Antarctic Bottom Water in the Abyssal Ocean*, Journal of Physical Oceanography **46** (2016), 635–661.

[3] C. Wunsch, *On oceanic boundary mixing*, Deep Sea Research and Oceanographic Abstracts **17** (1970), 293–301.

[4] O. M. Phillips, *On flows induced by diffusion in a stably stratified*, Deep Sea Research and Oceanographic Abstracts **17** (1970), 435–443.

[5] S. A. Thorpe, *Current and Temperature Variability on the Continental Slope*, Philosophical Transactions of the Royal Society of London A: Mathematical, Physical and Engineering Sciences **323** (1987), 471–517.

[6] C. Garrett, P. MacCready, P. B. Rhines, *Boundary Mixing and Arrested Ekman Layers: Rotating Stratified Flow Near a Sloping Boundary*, Annual Review of Fluid Mechanics **25** (1993), 291–321.

[7] J. Callies, *Restratification of Abyssal Mixing Layers by Submesoscale Baroclinic Eddies*, Journal of Physical Oceanography **48** (2018), 1995–2010.

[8] H. G. Peterson, J. Callies, *Rapid Spinup and Spindown of Flow along Slopes*, Journal of Physical Oceanography **52** (2022), 579–596.

[9] H. G. Peterson, J. Callies, *Coupling between Abyssal Boundary Layers and the Interior Ocean in the Absence of Along-Slope Variations*, Journal of Physical Oceanography (in press).

Numerical phase averaging for geophysical fluid dynamics

Colin Cotter

(joint work with Werner Bauer, Beth Wingate, Hiroe Yamazaki)

We consider highly oscillatory PDEs of the form

$$U_t = LU + N(U), \tag{1}$$

where L is a skewsymmetric operator leading to high frequency oscillation, and N is some nonlinear operator. Following many works, including [4, 6], we define the modulated variable

$$V(s,t) = \exp(-L(s+t))U(t), \tag{2}$$

where s is a phase parameter. Then,

$$V_t(s,t) = \exp(-L(s+t))N(\exp(L(s+t)V(t))). \tag{3}$$

In this form, the fast dynamics is transformed into a fast nonautonomous time dependence in the tendency.

A phase average of these equations over s leads to

$$\bar{V}_t = \lim_{T\to\infty} \int_{-T}^{T} \exp(-L(s+t))N(\exp(L(s+t)\bar{V}(t)))\mathrm{d}s. \tag{4}$$

The infinite integral is necessary when L has a set of eigenvalues with no greatest common multiple, i.e. solutions of $U_t = LU$ are quasiperiodic. [4] showed that for the rotating shallow water equations, applying this procedure followed by taking the limit of small Rossby number leads to solutions of the quasigeostrophic equations. [2] translated this idea to a numerical scheme in two steps. First, a finite averaging window T is chosen, and a smooth kernel function is introduced to obtain

$$\bar{V}_t = \int_{-T}^{T} \rho(s/T) \exp(-L(s+t)) N(\exp(L(s+t)\bar{V}(t))) \mathrm{d}s. \tag{5}$$

Second, the integral is replaced by a quadrature sum, whose terms can be evaluated independently on a parallel computer.

$$\bar{V}_t = \sum_{i=1}^{N} w_i \exp(-L(s_i+t)) N(\exp(L(s_i+t)\bar{V}(t))), \tag{6}$$

where $\{w_i\}_{i=1}^N$ are quadrature weights and $\{s_i\}_{i=1}^N$ are quadrature points. For small T, we recover the original equations, and for large T, we obtain filtered equations that damp oscillatory components of the right hand side. When integrating these equations with a numerical timestepper, this allows for larger timesteps with smaller error (versus an exact solution of the phase averaged ODE) and potentially enhanced stability. It is also interesting to consider the contributions to the slow dynamics of near resonances between fast frequencies of L that are neglected when $T \to \infty$. This technique requires a method of implementing the action of matrix exponentials. The REXI (rational approximation of exponential integrators) approach [7] is one promising technique that uses parallel solution of independent linear systems of the form $a_i I + b_i L$. These systems have the same structure as the systems that arise from implicit timestepping of $U_t = LU$, but with complex valued timesteps. The iterative solution of these systems have challenges but if these are overcome, this approach has the potential to yield evaluations of the action of $\exp(tL)$ with t-independent wallclock times.

[2] used the averaging technique to construct a coarse propagator for a time-parallel "parareal" iteration, but it is useful to consider the averaged timestepper as a useful numerical integrator in its own right. In [8], we examined the time integration error in a phase averaged integrator, i.e. the error versus the exact solution of the ODE obtained after spatial discretisation, when applied to a standard testcase for the rotating shallow water equations on the sphere. This testcase contains both fast inertia-gravity waves and slow balanced dynamics. We found that for fixed Δt, there is an optimal T that compromises between numerical timestepping error and phase averaging error (as analysed in [5]). We also found that the error is much less than the error obtained when applying a standard semiimplicit time integrator to the original equations with the same Δt. Unfortunately, we were not able to extend Δt beyond the range possible with the semiimplicit method as hoped, because of instability. We believe this to be due to CFL constraints from N itself (the testcase does not have a very large timescale separation), and we are currently looking into moving more of N into L (perhaps dynamically).

For very large timesteps, the averaging error dominates, and so we are interested in reducing this error via predictor-corrector techniques. This requires a hierarchy of approximations. One way to construct such hierarchies is to consider (4) as a projection (with respect to an appropriate norm) of (3) onto the subspace of functions $V(s,t)$ that are constant in s. [1] introduced the idea of creating more accurate approximations by expanding in a basis in s. They considered a simple example of a polynomial basis, and demonstrated exponential convergence to the exact solution when applied to the case of the swinging spring with 2:1 resonance [3]. However, with that basis, the convergence is still very slow for T larger than the time period of the fast frequency. In more recent work we have been examining expansion in the basis $\{\exp(ksL)\}_{k=0}^{K}$, which shows fast convergence even for large T. We have a pathway towards an efficient and scalable implementation of this idea for geophysical fluid PDEs as a deferred correction scheme, using the standard averaging method as the "coarse propagator". This is the focus of our current work in this direction.

References

[1] W. Bauer, C. J. Cotter and B. Wingate, *Higher order phase averaging for highly oscillatory systems*. Multiscale Modelling and Simulation **20(3)**, (2022), 936–956.

[2] T. S. Haut, T. Babb, P. Martinsson and B. Wingate, *A high-order time-parallel scheme for solving wave propagation problems via the direct construction of an approximate time-evolution operator*, IMA Journal of Numerical Analysis **36**, (2016), 688–716.

[3] D. D. Holm and P. Lynch, *Stepwise precession of the resonant swinging spring*, SIAM Journal on Applied Dynamical Systems **1**, (2002), 44–64.

[4] A. J. Majda and P. Embid, *Averaging over fast gravity waves for geophysical flows with unbalanced initial data*, Theoretical and Computational Fluid Dynamics **11**, (1998), 155–169.

[5] A. .G. Peddle and T. Haut, B. Wingate, *Parareal convergence for oscillatory PDEs with finite time-scale separation*. SIAM Journal on Scientific Computing (2019), **41**, A3476–A3497.

[6] S. Schochet, *Fast singular limits of hyperbolic PDEs*. Journal of Differential Equations (1994), **114**, 476–512.

[7] M. Schreiber, M., P. .S. Peixoto, T. Haut and B. Wingate, *Beyond spatial scalability limitations with a massively parallel method for linear oscillatory problems*. The International Journal of High Performance Computing Applications (2018), **32**,913–933.

[8] H. Yamazaki, C. J. Cotter and B. Wingate, *Time parallel integration and phase averaging for the nonlinear shallow water equations on the sphere*, arXiv preprint arXiv:2103.07706.

Asymptotic modeling of ice nucleation due to gravity waves

Stamen I. Dolaptchiev

(joint work with Peter Spichtinger, Manuel Baumgartner, Ulrich Achatz)

Cirrus clouds are high-altitude ice clouds in the atmosphere. Those clouds are a major source of uncertainty in the climate system modeling. One reason for this is the multi-scale nature of the interactions between dynamics and cloud physics. For example, propagating gravity waves (GW) can induce nucleation of new ice crystals, which eventually will form a cirrus cloud. The number and the size of the

nucleated ice crystals crucially depend on the properties of the GW. The ice crystal number and size further affect the radiative response of the cirrus by modifying the delicate balance between the reflection of incoming solar radiation and the absorption of outgoing long-wave radiation. The complex interactions between GW and cirrus are poorly represented in current climate models.

Here we apply an asymptotic framework to identify systematically the dominant interactions between the GW and cirrus clouds. In particular, we focus on homogeneous nucleation of in situ cirrus in the tropopause region. The clouds are described using a double-moment bulk ice microphysics scheme including effects due to sedimentation, nucleation and diffusional growth. The GWs considered are mid-frequency GWs close to breaking due to static instability. The time scale of such waves is comparable with the time scale of diffusional growth of the ice crystals. First, in the asymptotic approach the governing equations for the GW dynamics and for the ice physics are nondimensionalized using reference quantities describing the mid-frequency GW and tropopause cirrus. Next, all nondimensional characteristic numbers are expressed in terms of a small parameter ϵ. This small parameter can be interpreted as the ratio between the GW vertical scale and the pressure scale height, and ϵ can be related to a nucleation exponent, as well. With this small parameter an asymptotic expansion is performed allowing to derive self-consistent reduced equations describing ice nucleation forced by a passing GW.

Further, solutions of the reduced equations are derived using the matched asymptotic approach of [1]. The dynamics is subdivided into three different regimes: a pre- and post-nucleation regimes, characterized by the slow diffusional growth time scale, and a nucleation regime on a much faster nucleation time scale. Analytical solutions are found for the three regimes and a composite solution is constructed by matching the different solutions. This allows to make a prediction of the final number concentration of nucleated ice crystals, N_{post}, which is given by the expression

$$N_{post} = \begin{cases} \frac{2A^* S_c \cos(\omega t_0 + \phi)}{D^*(S_c - 1)} - N_{pre} & N_{pre} < \frac{A^* S_c \cos(\omega t_0 + \phi)}{D^*(S_c - 1)} \\ N_{pre} & else \end{cases}, \tag{1}$$

where A^* is proportional to the GW vertical velocity amplitude, ω is the GW frequency, S_c is a critical saturation ratio for the onset of nucleation, D^* is a deposition coefficient and N_{pre} denotes the initial number concentration. Interestingly, equation (1) provides an upper bound of nucleated ice crystals for fixed vertical velocity, as well as, a threshold for the initial number of ice crystals, which will inhibit nucleation. To our knowledge current parameterizations of ice nucleation due to GWs are lacking of such physical constrains.

Using numerical simulations of the reduced ice physics model, capturing the effects of nucleation and diffusional growth, it is demonstrated that the asymptotic solution (1) provides very precise approximation of the nucleation events. In addition, the dependence of the nucleated ice crystal number concentration on

the initial GW phase ϕ is analyzed. Implications of the results for high- and low-frequency GWs, as well as, for the construction of novel cirrus parameterizations in climate models are discussed.

References

[1] M. Baumgartner and P. Spichtinger, *Homogeneous nucleation from an asymptotic point of view*, Theor. Comput. Fluid Dyn. **33** (2019), 83–106.

Ekman-inertial instability

Nicolas Grisouard

(joint work with Fabiloa Trujano-Jiménez, Varvara E. Zemskova)

Submesoscale flows are characterised by relative vertical vorticities ζ that are comparable in magnitude to the planetary vorticity, also known as the Coriolis parameter f. This ratio can define a local Rossby number $\mathrm{Ro} = \zeta/f = O(1)$. At mid-latitudes, this number translates into vortices or jets that are on the order of 1 to 100 km wide. Submesoscale flows have somewhat large vertical velocities, which play a significant role in e.g. air-sea exchanges, marine ecosystems, and dissipation of kinetic energy [1].

Fluid instabilities often mediate these phenomena. In particular, so-called inertial instabilities occur when the condition $\mathrm{Ro} < -1$ is met somewhere along a jet. They manifest themselves as horizontal flows that grow exponentially at a rate $F = f\sqrt{|1 + \mathrm{Ro}|}$. When such a perturbation originates at the ocean surface (for example due to a change in wind conditions) rather than noise in the volume, a type of non-normal instability can arise, which we call "Ekman-inertial instability" (EII) [2]. First, the wind stress is communicated to the interior of the ocean via viscous stresses, as in a Stokes problem. This initial viscous entrainment is very efficient in setting horizontal layers of fluid in motion, so that if the perturbation occurs rapidly enough, the initial growth rate can far exceed the nominal growth rate F. After this initial, potentially rapid growth, the layer, in turn, entrains the layer immediately below. The horizontal velocity of the former layer continues to grow, although at a rate that is now lower than F. As momentum homogenises vertically, the growth rate asymptotically increases back to F. The process repeats at depth, layer-by-layer, until saturation.

The strong growth rate of EII might paradoxically make it hard to diagnose in models or observations. In fact, rapid homogenisation of anticyclonicity could "kill the patient" too quickly to observe. However, this could provide an explanation for why the values of ζ/f below -1 are very rare, even though direct diagnostics of inertial instability are rare [3].

EII is the unstable counterpart to the establishment of an Ekman spiral and its accompanying inertial oscillations when $\mathrm{Ro} > -1$. In other words, there cannot be Ekman layers or inertial oscillations when $\mathrm{Ro} < -1$.

Regions where $\mathrm{Ro} < -1$ usually occur in the flanks of density fronts, i.e., regions of strong lateral buoyancy gradients. These gradients represent reservoirs

of available potential energy. The horizontally flowing EII can advect such lateral buoyancy gradients as passive tracers, tapping into the potential energy of the front. This represents a significant departure from several instabilities such as the symmetric or "traditional" inertial instabilities: they primarily flow along isopycnals, and their energetic footprint is usually seen as primarily extracting kinetic energy from the front's jet. That EII could tap into the available potential energy budget of the front may explain our previous results [5].

More broadly, the capacity of the EII to horizontally advect isopycnals is also found in the model of "Turbulent thermal wind" (TTW), whereby Ekman transport, modified by thermal wind shear, can in some cases create a horizontal convergence of isopycnals, that is, frontogenesis [6]. TTW and EII are fundamentally different in that the former is stable and driven ($\mathrm{Ro} > -1$), while EII is self-sustained. However, they may be hard to distinguish without a careful investigation of the momentum balance of a given situation.

When fronts have finite widths, horizontal convergences create vertical divergences and early saturation of EII. Vertical motions then take the form of either slowing evolving pumping and suction and/or internal waves. While pumping and suction also accompany during the establishment of an Ekman layer and of a "traditional" inertial instability, the more rapid evolution of EII is correlated with more energetic and higher-frequency internal waves.

References

[1] J. C. McWilliams, *Submesoscale currents in the ocean*, Proc. R. Soc. Lond. A **472**, 20160117
[2] N. Grisouard, V. E. Zemskova, *Ekman-inertial instability*, Phys. Rev. Fluids **5** (2020), 124802
[3] A. Y. Shcherbina, E. A. D'Asaro, C. M. Lee, J. M. Klymak, M. J. Molemaker, J. C. McWilliams, *Statistics of vertical vorticity, divergence, and strain in a developed submesoscale turbulence field*, Geophys. Res. Lett. **40**, 4706–4711
[4] L. N. Thomas, J. R. Taylor, R. Ferrari, T. M. Joyce, *Symmetric instability in the Gulf Stream*, Deep-Sea Res. II **91** (2013), 96-110
[5] N. Grisouard, *Extraction of Potential Energy from Geostrophic Fronts by Inertial-Symmetric Instabilities*, J. Phys. Oceanogr. **48** (2018), 1033-1051
[6] J. C. McWilliams, *Oceanic Frontogenesis*, Annu. Rev. Mar. Sci. **13** (2021), 227-253

Learning Data-driven Subgrid-Scale Models for Geophysical Turbulence: Stability, Extrapolation & Interpretation

Pedram Hassanzadeh

There is a growing need for more accurate and faster climate and weather models to better project climate change and forecast extreme weather. However, the atmospheric and oceanic turbulent circulations involve a variety of nonlinearly interacting physical processes spanning a broad range of spatial and temporal scales (form a few centimeters and smaller to tens of thousands of kilometer). To make simulations of these turbulent flows computationally tractable, processes with scales smaller than the typical grid size of weather/climate models ($\sim$ 100 km) have to be parameterized. Recently, there has been substantial interest (and progress) in

using deep learning techniques to develop data-driven subgrid-scale (SGS) parameterizations for a number of key processes in the atmosphere, ocean, and other components of the climate system. However, for these data-driven SGS parameterizations to be useful and reliable in practice, a number of major challenges have to be addressed. These include: 1) instabilities arising from the coupling of data-driven SGS parameterizations to coarse-resolution solvers, 2) learning in the small-data regime, 3) interpretability, and 4) extrapolation to different parameters and forcings.

We have used several setups of 2D turbulence and Rayleigh-Benard convection as test cases to introduce methods to address (1)-(4). These methods are based on combining turbulence physics and recent advances in theory and applications to deep learning. For example, we use backscattering analysis to shed light on the source of instabilities [1] and incorporate physical constraints to enable learning in the small-data regime. We discuss incorporating these constraints, such as symmetries and conservation laws, through the neural network architecture and/or through a customized loss function [2].

We further introduce a novel framework based on spectral (Fourier) analysis of the neural network to interpret the learned physics [3]. This explainability framework reveals that deep convolutional neural networks (CNNs) learn low- and high-pass filters, as well as Gabor filters, when applied to SGS modeling of geophysical turbulence. Finally, we show how transfer learning enables neural networks to extrapolate in parameters, e.g., by a factor of 100 in Reynolds number. Transfer learning involves targeted re-training of an already-trained neural network using new data, and is becoming a powerful and popular tool in scientific machine learning. Applying the explainability framework shows that transfer learning has learned new filters consistent with how the physics of the flow change as the Reynolds number is increased.

Putting all results together, we demonstrate how issues (1)-(4) can be addressed in supervised learning of SGS models for geophysical turbulence. Next steps in applying these ideas to more complex phenomenon, e.g., gravity waves in the atmosphere, and potential challenges and solutions are discussed. More broadly, this work provides a new avenue for optimal and explainable transfer learning, and a step toward fully explainable deep neural networks, for wide-ranging applications in science and engineering, such as climate change modeling.

References

[1] Y. Guan, A. Chattopadhyay, A. Subel and P. Hassanzadeh, *Stable a posteriori LES of 2D turbulence using convolutional neural networks: Backscattering analysis and generalization to higher Re via transfer learning*, Journal of Computational Physics, **458** (2022).

[2] Y. Guan, A. Subel, A. Chattopadhyay, and P. Hassanzadeh, *Learning physics-constrained subgrid-scale closures in the small-data regime for stable and accurate LES*, under review, https://arxiv.org/abs/2201.07347

[3] A. Subel, Y. Guan, A. Chattopadhyay, and P. Hassanzadeh, *Explaining the physics of transfer learning a data-driven subgrid-scale closure to a different turbulent flow*, under review https://arxiv.org/abs/2206.03198

Computing Lagrangian means without tracking particles

Hossein Kafiabad
(joint work with Jacques Vanneste)

Time averaging is one of the most essential tools in analysing fluid flows with multiple time scales, which are ubiquitous in nature and industries. A prominent use of time averaging is the flow decomposition into fast and slow parts to understand different phenomena associated with each time scale. For instance, in geophysical flows the wave dynamics is associated with the fast part, and the slow dynamics can be reduced to a balance between a few forces (geostrophic and hydrostatic balance). Another application of time averaging is to filter out the fast variations that are not fully captured in numerical simulations or observations to make meaningful inferences from the remaining slow dynamics. Similarly, the noise and error inherent in measurements or simulations are removed by averaging.

For fluids, time-averaging can be performed in two different ways. The most straightforward approach is to average time series of flow variables at fixed spatial points, to obtain the so-called Eulerian mean (EM). Another approach is to average flow variables along particle trajectories instead of fixed positions, which gives the Lagrangian mean (LM). Lagrangian averaging has several pivotal advantages over its Eulerian counterpart as illustrated by a growing number of studies. For instance, it removes the Doppler shift that eclipses the separation of time scales between the background flow and waves. However, the widespread adoption of Lagrangian averaging has been hindered by computational complications. To compute the LM in numerical models usually particles are tracked using interpolated velocities at particle positions at every time steps. This is a computational challenge that requires extra memory space (considering time series of variables are stored at all grid points) and is ill-suited for efficient computational parallelisation.

We propose a numerical approach that circumvents these difficulties. This new approach is based on the evolution of partial means instead of particle tracking. Partial means can be viewed as means over shorter intervals than the total averaging period. In this approach, we compute the LMs as solutions to a set of Partial Differential Equations (PDEs) that describe the evolution of these partial means. This paradigm could be a breakthrough in computing LMs as these PDEs can be discretised in a variety of ways and solved on-the-fly (i.e. simultaneously with the dynamical governing equations). Hence, they do not require storing any time series and substantially reduce the memory footprint compared to particle tracking.

We offer two strategies in this approach (see [2]), where each strategy has its own advantages. The first, which generalises the algorithm of [1], uses end-of-interval particle positions; the second directly uses the Lagrangian mean positions. We briefly review the strategy 2 of this paper to provide a gist of this approach. We denote the (generalised) LM of the field f by $\bar{f}^L(\mathbf{x}, t_0, t)$, where the averaging is performed from t_0 to t and $\mathbf{x}$ is the mean position of the particle over this interval. We also define the displacement field $\xi(\mathbf{x}, t_0, t)$ such that $\mathbf{x} + \xi(\mathbf{x}, t_0, t)$ is

the current position of the particle at t. Starting from the definition of LM, the following coupled PDEs are derived:

$$(1)\quad \partial_t \bar{f}^L(\mathbf{x},t_0,t) + \frac{\xi(\mathbf{x},t_0,t)}{t-t_0}\cdot\nabla\bar{f}^L(\mathbf{x},t_0,t) = \frac{f(\mathbf{x}+\xi(\mathbf{x},t),t_0,t)-\bar{f}^L(\mathbf{x},t_0,t)}{t-t_0},$$

$$(2)\qquad \partial_t \xi(\mathbf{x},t_0,t) + \frac{\xi(\mathbf{x},t_0,t)}{t-t_0}\cdot\nabla\xi(\mathbf{x},t_0,t) = \mathbf{u}(\mathbf{x}+\xi(\mathbf{x},t),t_0,t) - \frac{\xi(\mathbf{x},t_0,t)}{t-t_0}.$$

If the desired averaging period is T, these PDEs should be integrated from t_0 to t_0+T to get the LM for this period. At intermediate time steps ($t_0 < t < t_0+T$), the above equation describes the evolution of partial means, which are the means for intervals shorter than the ultimate averaging period. Note that in these PDEs t_0 can be treated as a fixed parameter, which is related to the slow-time variation of LM fields. These equations can be discretised in a variety of ways depending on the application and the nature of the problem.

References

[1] Kafiabad, H., *Grid-based calculation of Lagrangian mean*, Journal of Fluid Mechanics, **94** (1990).

[2] Kafiabad, H & Vanneste, J., *Computing Lagrangian means*, submitted to Journal of Fluid Mechanics, (arXiv preprint arXiv:2208.02682).

Parameterization of non-orographic gravity waves in large-scale models. Formalism, impact and test against direct observations.

Francois Lott

The parameterization of non-orographic gravity waves breaking in the atmospheric component of the large scale Coupled Model developed at IPSL for the 6th IPCC assessment report (IPSLCM6) will be reviewed. For the gravity waves emitted by front [5, 2] show that the GW sources can be derived from spontaneous adjustment theory, providing that the sources are placed at multiple altitudes in the troposphere and lower stratosphere. The representation of gravity waves issued from convection in [6] is derived from a much simpler theory, where the variability of the latent heating due to convection is distributed over a large ensemble of spatio-temporal harmonics each harmonic forcing the corresponding waves. In these two different schemes, the large ensemble of waves needed is realised by stochastic methods.

The parameterizations are shown to reduce systematic errors, for instance on the quasi-biennal oscillation in the tropical stratosphere or on the timing of the final warming in the southern hemisphere middle atmosphere [4]. In this respect careful diagnostics are also made of the large scale equatorial waves, and to verify that the parameterizations are not spuriously balancing errors on element of dynamics that should be explicitly solved by the model [3].

Finally, [1] presents direct comparison with constant level balloon flights done in November 2019-February 2020 and in the lower tropical stratosphere during the strateole-2 campaign. The atmospheric conditions under the balloons location at each time are derived from the ERA5 re-analysis and used to activate the non-orographic gravity waves schemes. We show that the momentum fluxes predicted by the schemes compare well with the observed values, and with highly significant correlations between the day-to-day variabilities. The correlations obtained are for the operational values of the non-dimensional "tuning" parameters of the schemes, and have values that could be well improved, regarding the number of degrees of freedom present in the dataset.

References

[1] F. Lott, R. Rani, A. Podglagen, F. Codron, A. Hertzog, and R. Plougonven, *Direct comparison between a non orographic gravity wave drag scheme and constant level balloons*, (2022) submitted to Journal of Geophysical Research.

[2] B. Ribstein, C. Millet, F. Lott, and A. de la Camara, *Can we improve the realism of gravity wave parameterizations by imposing sources at all altitudes in the atmosphere?* J. Adv. Model. Earth Systems, **(14)**, (2022) e2021MS002563. https://doi.org/10.1029/2021MS002563.

[3] L. A. Holt, F. Lott, and co-authors, *An evaluation of tropical waves and wave forcing of the QBO in the QBOi models*, (2020) Quart. J. Roy. Meteor. Soc., doi:10.1002/qj.3827.

[4] A. de la Camara, and F. Lott, and M. Abalos, *Climatology of the middle atmosphere in LMDz: Impact of source-related parameterizations of gravity wave drag*, (2016), J.Adv. Model. Earth Systems, DOI: 10.1002/2016MS000753.

[5] A. de la Camara and F. Lott, *A parameterization of gravity waves emitted by fronts and jets,* **(42)**(2015), Geophys. Res. Letters, doi:10.1002/2015GL063298.

[6] F. Lott and L. Guez, *A stochastic parameterization of the gravity waves due to convection and impact on the equatorial stratosphere,*, J. Geophys. Res. **(118, 16)** (2013), 8897-8909. DOI: 10.1002/jgrd.50705.

Inertial wave attractor induced mean flow and vortex cluster

Leo Maas

Recently, a vortex cluster emerged in a lab and related numerical experiment [1], 2021). This cluster was found by pure serendipity, as we applied axisymmetric, periodic forcing at the lid of an annulus that was filled with a homogeneous-density, uniformly rotating fluid. Owing to the presence of a conical bottom, we anticipated finding an axisymmetric inertial wave attractor, aiming to investigate the attractor?s role in the generation of a cyclonic mean flow. This mean flow did develop, but displayed an ill-understood subsequent evolution. Unexpectedly, it led to a cluster of cyclonic vortices, that slowly migrate cyclonically. This cluster resembles the eight vortices encircling the central North polar vortex at Jupiter (however, here in a homogeneous-density fluid).

Interest in this problem was preceded by numerical computations in a similar set-up [3]. It showed that Triadic Resonance Instabilities (TRI) occurred, and revealed

that at large forcing a breaking of an axisymmetric response may occur, preceding a transition to 3D turbulence.

That paper itself followed up on an earlier experimental paper [2] in which an inertial wave attractor was forced by libration of an eccentrically-positioned rectangular tank having a sloping side wall. It showed that a strong cyclonic mean-flow developed above the location where the attractor reflected from the sloping wall. This was heuristically interpreted as showing evidence of mixing, following the overturning of the radial stratification in angular momentum (due to breaking of focused and amplified inertial waves, locally violating Rayleigh?s stability criterion).

This talk will address the role of the cyclostrophic equilibrium, its perturbation, giving rise to an inertial wave attractor that together with its free (TRI-induced) and forced harmonics might lead to the generation of both an azimuthal as well as meridional mean flow. The meridional flow contains a strong downdraught above the focused attractor branch. It is expected to stretch background vortex lines, enhancing cyclonic vorticity. Instability of the axisymmetric mean flow that is generated may possibly lead to a combination of an axisymmetric cyclonic mean flow and Topographic Rossby Waves (TRWs), together featuring as the slowly migrating vortex cluster.

References

[1] S. Boury, I. Sibgatullin, E. Ermanyuk, N. Shmakova, P. Odier, S. Joubaud, L.R.M. Maas, T. Dauxois, *Vortex cluster arising from an axisymmetric inertial wave attractor*, Journal of Fluid Mechanics **926** (2021), A12-1–36.

[2] L.R.M. Maas, *Wave focusing and ensuing mean flow due to symmetry breaking in rotating fluids*, Journal of Fluid Mechanics textbf437 (2001), 13–28.

[3] I. Sibgatullin, E. Evgeny, L.R.M. Maas, X. Xu, T. Dauxois, *Direct numerical simulation of three-dimensional inertial wave attractors*, **In:** Ivannikov ISPRAS Open Conference (ISPRAS) IEEE (2017), 137–143.

New perspectives on the wave drag and pseudo-momentum flux of the oceanic internal tide

Callum Shakespeare

(joint work with Brian K. Arbic, Andy McC. Hogg)

Wave drag and wave momentum flux are key parameters for the understanding and parameterising the impact of internal waves on the balanced flow. The wave drag is, loosely, the force exerted by waves on their generating flow whereas the (pseudo-)momentum flux is the momentum carried by the waves which is deposited where they dissipate. In the classical model of steady mean flow over a hill generating internal lee waves, these two parameters are equivalent: the divergence of the wave momentum flux equals the wave drag. In recent years, oceanographers have mistakenly assumed an analogous paradigm for the generation of internal tides by an oscillatory mean flow. However, the oscillatory case is a far more

complex situation. Firstly, for a purely oscillatory flow, the generation of equal and opposite internal tide beams leads to zero net momentum flux. Indeed, an internal tide equivalent to the lee wave momentum flux only exists in the presence of a steady component to the mean flow (in addition to the oscillatory), which Doppler shifts the internal tide beams, resulting in enhanced upstream and diminished downstream momentum flux [3]. As for lee waves, the divergence of this spatial-mean flux is associated with a wave drag on the steady component of the mean flow. However, when oceanographers talk about internal tide 'wave drag' they are referring to something else entirely; namely, the oscillatory topographic stress associated with the generation of the internal waves. This stress is not directly related to the momentum or energy flux of the waves, and exists even for evanescent waves when those fluxes are identically zero [1]. Furthermore, unlike steady wave drag which acts where waves dissipate, the oscillatory wave drag acts in the topographic boundary layer [2]. Thirdly, in the oscillatory problem, it is not only the spatial-mean momentum flux that is relevant; the flux associated with each individual internal tide beam is important even if the spatial-mean is zero. The deposition of the beam momentum flux can locally accelerate the flow, but with an equal and opposite acceleration occurring elsewhere due to the second beam. In this way, the internal tide is able to energise counter-flowing balanced currents such as eddies or jets, without driving a spatial-mean flow [4]. There is a need to parameterise all three of these effects (i.e. steady wave drag, oscillatory wave drag, beam momentum flux) in numerical ocean models, but this has largely not been done to date. However, the physical understanding developed in the present work provides a first step in this direction.

References

[1] C. J. Shakespeare, B. K. Arbic and A. McC. Hogg, *The Drag on the Barotropic Tide due to the Generation of Baroclinic Motion*, Journal of Physical Oceanography **30.12** (2020), 3467-3481.

[2] C. J. Shakespeare, B. K. Arbic and A. McC. Hogg, *The Impact of Abyssal Hill Roughness on the Benthic Tide*, Journal of Advances in Modeling Earth Systems**13.5** (2021), e2020MS002376.

[3] C. J. Shakespeare, *Interdependence of internal tide and lee wave generation at abyssal hills: Global calculations*, Journal of Physical Oceanography**50.3** (2020), 655-677.

[4] C. J. Shakespeare and A. McC. Hogg, *On the momentum flux of internal tides*, Journal of Physical Oceanography **49.4** (2019), 993-1013.

How does wave field evolution drive surface ocean currents?

Victor I. Shrira

(joint work with Sergei I. Badulin, Rema Almelah)

In the context of atmosphere–ocean interaction the role played by wind waves is one of the key outstanding problems of obvious huge significance. It has been long known that wind waves and surface currents are intricately linked in many different ways. Historically, the lion share of attention has been given to effects of currents

on waves. Here we focus on the poorly studied effect of waves on currents. It has been realized in the seventies that in the rotating ocean wind waves are exerting substantial Reynolds shear stresses and, thus, can strongly affect surface currents ([Hasselmann(1970)]). A mathematical framework for dynamics of surface currents accounting for both the wind and wave stresses was formulated by [Huang(1979)]: the corresponding equations are referred to as the *Stokes-Ekman model*, since the wave field affects currents via its Stokes drift. On the basis of this model, under the oversimplifying assumptions of steady or "frozen" wave field, it was found that the effect of wave stresses can be indeed quite substantial, but no further steps were made.

The classical Ekman model totally ignores waves. [Shrira & Almelah(1979)] derived the general solution of the Stokes-Ekman model for time dependent wind and wave field, allowing the eddy viscosity to depend both on time and depth. The most recent trend is to consider coupled models of wave dynamics (e.g. Wavewatch III) and ocean circulation (e.g NEMO, [Couvelard *et al.*(2020)]). However, the use of such models is prohibitively expensive.

Here, we first examine analytically the surface current response to both wind and evolving wind-wave field within the Stokes-Ekman paradigm in its simplest setting – assuming constant eddy viscosity. One of the key points of this work is that wind-wave fields cannot be treated as frozen, since wave fields continue to evolve whatever behaviour of the wind. The focus of the study is on the effect of presumed to be known wave-field evolution on currents. At present, even the most basic questions, like, whether the wind and wave induced current grows or decays under a constant wind, remain totally open.

The established statistical theory of wave field dynamics based upon the Hasselmann equation predicts self-similar large-time asymptotics of wind-driven seas with rigidly linked magnitudes and rates of wave growth (see e.g. [Badulin *et al.* (2007)]). This implies a linkage of the magnitudes and vertical scales of the wind and wave induced surface currents. Thus, the dynamics of surface currents should be determined by the regimes of wave field evolution. By solving analytically the Stokes-Ekman equation we find how the surface currents are driven by the wave field. In particular, we find under what circumstances the wave-induced current component exceeds the wind-induced one and when it is the dominant factor. We establish how the vertical structure of the surface current evolves. We show that under steady wind the large time asymptotics is determined by the regime of the wave field evolution: for "young waves" the surface current grows with time to infinity, while, in contrast, for "old waves" it asymptotically decays. Since the wave field and its contribution to surface current evolve, at large scale the surface current becomes spatially nonuniform, we find analytically its curl and divergence, which enables us to quantify how waves affect deep ocean currents via the Ekman pumping/suction.

References

[Badulin *et al.* (2007)] Badulin, S. I., Babanin, A. V., Resio, D. & Zakharov, V. *Weakly turbulent laws of wind-wave growth.* J. Fluid Mech. **591** (2007), 339–378.

[Hasselmann(1970)] Hasselmann, K. *Wave-driven inertial oscillations.* Geophysical Fluid Dynamics **1** (3-4) (1970), 463–502, https://doi.org/10.1080/03091927009365783.

[Huang(1979)] Huang, N. E. *On surface drift currents in the ocean.* J. Fluid Mech. **91** (1) (1979), 191–208.

[Shrira & Almelah(1979)] Shrira, V. I. & Almelah, R. B. *Upper-ocean Ekman current dynamics: a new perspective* . J. Fluid Mech., **887**, (2020), A24.

[Couvelard *et al.*(2020)] Couvelard, X., Lemarié, F., Samson, G., Redelsperger, J-L., Ardhuin, F., Benshila, R. & Madec, G. *Development of a two-way-coupled ocean-wave model: assessment on a global NEMO (v3.6)-WW3 (v6.02) coupled configuration.* Geosci. Model Dev. **13**, (2020), 3067-3090; https://doi.org/10.5194/gmd-13-3067-2020.

Modelling vertical mixing by statistical mechanics at a density interface

Joel Sommeria

(joint work with Hamed Vaziri, Antoine Venaille)

We present a statistical mechanics approach that models the vertical mixing in a density stratified fluid, relying on the previous work by [1]. This approach is compared to the classical hierarchical closure model of [2] for the buoyancy flux. Our model, based on a different physical approach, yields the probability distribution (pdf) of buoyancy values at each position, while the model of [2] is limited to its first moments. The results of the two approaches are closely related when the pdf is Gaussian, but they significantly differ otherwise.

We here focus on the case of turbulent mixing at the interface between a dense fluid and light fluid. The pdf is highly skewed away from the interface, so that our model significantly differs from those of [2]. Unlike them, it naturally accounts for the remarkable persistence of a sharp interface during the turbulent diffusion process. Indeed the energetic constraint tends to favor the sorting of fluid elements by density. The interface thickness results from a competition of this sorting effect with the stirring due to the kinetic energy input.

A net buoyancy flux however occurs through the interface, associated with irreversible mixing. If turbulence is produced in the lower part only, this results in a upward propagation of the interface, as it occurs in the laboratory context considered as the reference case: turbulence is generated by an oscillating grid, see figure below, left hand side. This irreversible mixing and associated vertical propagation are classically characterised by an entrainment coefficient E, which depends on a Richardson number Ri characterising the strength of the density stratification. Our model properly reproduces laboratory results, as shown in the graph on the right hand side of the figure. It however requires an appropriate splitting between internal wave perturbations and turbulence occuring at smaller scales. Only the latter contribution is properly described by our approach.

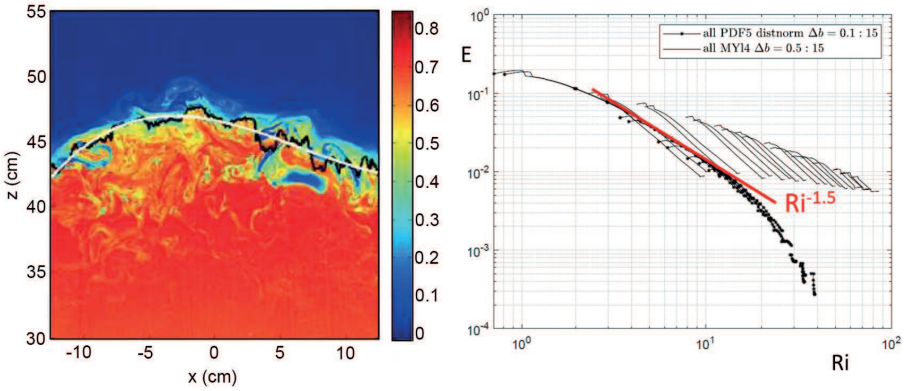

FIGURE 1. vertical cut of the buoyancy obtained experimentally by Laser Induced Fluorescence (left hand side) showing the turbulent interface between the lower fluid (buoyancy normalised to 0) and the upper one (buoyancy normalised to 1). The entrainment coefficient obtained by our model is compared to the empirical experimental law on the right hand side.

This approach relies on the general idea that turbulent stirring is a process of entropy increase, defined from an appropiate coarse grained description of the turbulent transport. Our model results from a principle of maximum entropy production consistent with the conservation of energy and other conserved quantities. A similar approach was previously applied to vorticity fluctuations in 2D or geostrophic turbulence, leading to the prediction of self-organisation into coherent vortices. It has been succesfully extended to the large scale organisation of 3D vortical flows [3]. Extensions to potential vorticity mixing could be fruitful. However the theoretical basis of the approach remains fragile because of the competition between turbulent stirring and irreversible cascade process toward small scales.

REFERENCES

[1] A. Venaille, L. Gostiaux, J. Sommeria, J., *A statistical mechanics approach to mixing in stratified fluids*, Journal of Fluid Mechanics. **810** (2017), 554-583.

[2] G.L. Mellor, T. Yamada, *Development of a turbulence closure model for geophysical fluid problems*, Reviews of Geophysics, **20** (1982), 851-875.

[3] S. Thalabard, B. Saint-Michel, E. Herbert, F. Daviaud, F., B. Dubrulle *A statistical mechanics framework for the large-scale structure of turbulent von Kármán flows*. New Journal of Physics, **17** (2015), 063006.

Monin-Obukhov Similarity Theory and its Generalization for Complex Atmospheric Turbulence

Ivana Stiperski
(joint work with Marc Calaf)

Atmospheric boundary layer turbulence provides a crucial coupling of the atmosphere, hydrosphere, cryosphere and biosphere in the climate system, and thus impacts all scales of atmospheric motions. In virtually all numerical models of atmospheric flows, this turbulent exchange between the Earth's surface and the overlying atmosphere is parametrized through the Monin-Obukhov similarity theory (MOST) [1]. MOST states that under the assumptions of horizontally homogeneous terrain and stationary flow conditions, a single length scale determined by surface fluxes of momentum and heat governs all turbulent exchange processes. Over the majority of the Earth's land surface, such as over complex terrain, however, these assumptions are clearly violated, and a viable theoretical description of turbulent exchange is missing. Still, for a lack of better alternative, MOST is widely used beyond its intended range of validity thus contributing to large uncertainty in weather, climate, and air-pollution models, particularly in polar regions and over mountains, both experiencing unprecedented warming.

The large parameter space of possible alternative influences on surface turbulent exchange and the difficulty of how to incorporate their many influences into MOST means that there has been little progress in extending MOST to complex terrain and addressing other of its limitation, a challenge that has plagued the community for decades. In our previous work [2, 3, 4, 5] we show that the complexity of the boundary conditions acting on turbulence is encoded in the anisotropy of the Reynolds stress tensor. The implications of this finding are addressed here through two examples: the formulation of a generalized extension of MOST based on anisotropy that successfully describes complex atmospheric turbulence, and the scalewise relaxation of turbulence towards an isotropic state at smallest scales shown to be universal and only dependent on bulk anisotropy.

The generalized extension of MOST, that encompasses a wide range of realistic surface and flow conditions, is formulated in the way that the directionality of turbulence exchange (degree of anisotropy computed from the invariants of the Reynolds stress tensor) is added as a key missing variable. The constants in the standard empirical MOST relations are shown to be functions of anisotropy, thus allowing a seamless transition between traditional MOST and its novel generalization. The new scaling relations, based on measurements from 13 well-known atmospheric datasets ranging from flat to highly complex mountainous terrain, show substantial improvements to scaling under all stratifications. The results also elucidate the role of anisotropy in explaining general characteristics turbulence that were so far missing from MOST, both over complex and canonical terrain, and for unstable and stable stratification, adding to the mounting evidence that anisotropy fully encodes the information on the complexity of the boundary conditions.

The question remains whether terrain influence on anisotropy persists to smaller scales so that the relaxation towards an isotropic state in complex terrain inherently differs from that over flat terrain. To answer this question, we examined the scalewise return-to-isotropy for 17 datasets collected above terrain ranging from flat to highly complex. The results show a strong nonlinearity of the trajectories causing significant departure from both, the linear Rotta [6] and other non-linear return-to-isotropy models. There is also a clear tendency of trajectories towards an axisymmetric state at smaller scale. Most importantly, however, results indicate that irrespective of the complexity of the dataset examined or thermal stratification, the return-to-isotropy trajectories that start from a specific limiting state of anisotropy show a surprising universality. This finding suggests that the effects of boundary conditions cease to be important at smaller scales. However, the scalewise route taken by the flow to wipe them out differs depending on the large-scale anisotropy set by the boundary conditions.

The exact way that the boundary conditions influence anisotropy is still an open topic. While it is known that anisotropy is strongly influenced by turbulence generation mechanisms such as shear, thermal stratification, and surface characteristics, over complex terrain there are a plethora of alternative processes related to terrain-induced pressure perturbations that can actively affect the anisotropy of the energy containing eddies. Hence, the frequency of occurrence of each of different states of anisotropy will be location-dependent. Understanding this connection between the boundary conditions and anisotropy is a crucial missing step to a viable parametrizations of turbulent exchange over complex terrain, to be addressed in my ERC CoG Grant "Developing a novel framework for understanding near-surface turbulence in complex terrain (Unicorn)".

References

[1] A.S. Monin, A.M. Obukhov, *Basic laws of turbulent mixing in the surface layer of the atmosphere*, Contrib. Geophys. Inst. Acad. Sci. USSR **24** (1954), 163–187.

[2] . Stiperski, M. Calaf, *Dependence of near-surface similarity scaling on the anisotropy of atmospheric turbulence*, Quarterly Journal of the Royal Meteorological Society **144** (2018), 641–657.

[3] I. Stiperski, M. Calaf,M. Rotach *Scaling, anisotropy, and complexity in near-surface atmospheric turbulence*, Journal of Geophysical Research: Atmosphere **124** (2019), 1428–1448.

[4] I. Stiperski, G. Katul, M. Calaf, *Universal return to isotropy of inhomogeneous atmospheric boundary layer turbulence*, Physical Review Letters **126** (2021), 194501.

[5] I. Stiperski, M. Chamecki, M. Calaf, *Anisotropy of unstably stratified near-surface turbulence*, Boundary-Layer Meteorology **180** (2021), 363–384.

[6] J. Rotta, *Statistische Theorie nichthomogener Turbulenz*, Zeitschrift für Physik **129** (1951), 547–572.

The Nonlinear Evolution of Internal Tides

Bruce R. Sutherland

Propagating in non-uniform stratification, the internal tide is known to excite superharmonics with double the horizontal wavenumber of the internal tide and nearly double the frequency [1]. If sufficiently large amplitude, the superharmonics can themselves excite superharmonics resulting in a cascade to successively larger horizontal wavenumber, and smaller horizontal scale. This is particularly true in the tropics, where the Coriolis parameter is small and the superharmonics are nearly resonant with the internal tide. This is demonstrated by way of theory, in the form of coupled ordinary differential equations, which predict that the superharmonic cascade leads to the formation of a solitary wave-train [2]. The results are in excellent agreement with fully nonlinear numerical simulations. For long waves in strong near-surface stratification, the results agree well with the prediction of shallow water theory including rotation through the Ostrovsky equation. The predictions of the Miyata-Choi-Camassa model including rotation are qualitatively similar, but less quantitatively accurate. This theory thus provides new insight into the dynamics leading to the nonlinear steepening of the internal tide, and it provides an efficient algorithm for predicting the evolution of the waves going beyond the restrictions of shallow water theory.

The internal tide and its superharmonics may also self-interact to produce horizontally long disturbances. Despite the transformation of the internal tide into solitary waves, the collective forcing by the parent wave and superharmonics is effectively steady in time. Thus we derive relatively simple formulae for the Stokes drift and induced Eulerian flow associated with the waves under the assumption that the parent waves and superharmonics are long compared with the fluid depth [3]. In all cases, the Stokes drift exhibits a mixed mode-1 and mode-2 vertical structure with the flow being in the waveward direction at the surface. If the background rotation is non-negligible, the vertical structure of the induced Eulerian flow is equal and opposite to that of the Stokes drift. This flow periodically increases and decreases at the inertial frequency with maximum magnitude twice that of the Stokes drift. When superimposed with the Stokes drift, the Lagrangian flow at the surface periodically changes from positive to negative over one inertial period. If the background rotation is zero, the induced Eulerian flow evolves non-negligibly in time and space for horizontally modulated waves: the depth below the surface of the positive Lagrangian flow becomes shallower ahead of the peak of amplitude envelope and becomes deeper in the lee of the peak. These predictions are well-captured by fully nonlinear numerical simulations.

References

[1] L. Baker & B. R. Sutherland, *The Evolution of Superharmonics Excited by Internal Tides in Non-uniform Stratification*, J. Fluid Mech. **891** (2020), R1.

[2] B. R. Sutherland & M. S. Dhaliwal, *The nonlinear evolution of internal tides. Part 1: The superharmonic cascade*, J. Fluid Mech. **948** (2022), A21.

[3] B. R. Sutherland & H. Yassin, *The nonlinear evolution of internal tides. Part 2: Lagrangian transport by periodic and modulated waves*, J. Fluid Mech. **948** (2022), A22.

Turbulent dynamics of the balanced flow in the ocean

Jim Thomas

The dominant share of oceanic flow kinetic energy resides in slowly evolving O(10-100) km scale geostrophically and hydrostatically balanced mesoscale eddies. Although rotation and density stratification supports many kinds of fast dispersive internal gravity waves in the ocean, these waves have been generically considered to be of much smaller spatial scales and energetically insignificant in comparison to balanced eddies. However, in situ, satellite altimeter, and realistically forced global scale ocean model outputs of the past one and half decade have challenged the previous notions of waves and balanced flow [4, 1, 3, 2]. Notably, recent datasets reveal that waves and balanced flow can have comparable spatial scales and energy levels. Furthermore, in certain oceanographic regions, internal waves can be more energetic than balanced flow in O(10-100) km scales. These findings have fuelled a broad set of research activities aimed at understanding how fast internal gravity waves affect the slowly evolving balanced component. Specifically, the oceanographic community has been keen in figuring out whether fast waves can form an energy sink for the slow balanced flow component. In this talk I will discuss theoretical and numerical results on wave-balance exchanges in the low Rossby number limit. Energy transfers between the balanced flow and three kinds of wave fields: wind generated near-inertial waves, low mode internal tides, and an internal wave continuum, will be discussed in detail with special emphasis on cases where waves can form an energy sink for balanced flow. More specific details of this work can be found in the references: [6], [7], [8], and [9].

References

[1] Torres, H. S. and Klein, P. and Menemenlis, D. and Qiu, B. and Su, Z. and Wang, J. And Chen, S. and Fu, L.-L. 2018 *Partitioning Ocean Motions Into Balanced Motions and Internal Gravity Waves: A Modeling Study in Anticipation of Future Space Missions*, J. Geophys. Res. Oceans **123** (2018), 8084–8105.

[2] Lien, R. C. and Sanford, T. B. *Small-Scale Potential Vorticity in the Upper Ocean Thermocline*, J. Phys. Oceanogr. **49** (2019), 1845–1872.

[3] Tchilibou, M. and Gourdeau, L. and Morrow, R. and Serazin, G. and Djath, B. and Lyard, F. *Spectral signatures of the tropical Pacific dynamics from model and altimetry: A focus on the meso/submesoscale range*, Ocean Science **14** (2018), 1283–1301.

[4] Savage, A.C. and Coauthers *Spectral decomposition of internal gravity wave sea surface height in global models*, J. Geophys. Res. Oceans **122** (2017), 7803–7821.

[5] Bühler, O. and Callies, J. and Ferrari, R. *Wave-vortex decomposition of one-dimensional ship-track data*, J. Fluid Mech. **756** (2014), 1007–1026.

[6] Thomas, J. and Yamada, R. *Geophysical turbulence dominated by inertia-gravity waves*, J. Fluid Mech. **875** (2019), 71–100.

[7] Thomas, J. and Arun, S. *Near-inertial waves and geostrophic turbulence*, Phys. Rev. Fluids **5** (2020), 014801.

[8] Thomas, J. and Daniel, D. *Turbulent exchanges between near-inertial waves and balanced flows*, J. Fluid Mech. **902** (2020), A7.

[9] Thomas, J. and Daniel, D. *Forward flux and enhanced dissipation of geostrophic balanced energy*, J. Fluid Mech. **911** (2021), A60.

Scattering of inertia-gravity waves by geostrophic flows

Jacques Vanneste
(joint work with M. R. Cox, M. A. C. Savva, H. A. Kafiabad)

Atmospheric and oceanic inertia-gravity waves (IGWs) propagate in complex, often turbulent flows in geostrophic and hydrostatic balance. This causes the continuous refraction of IGW energy and, as a result, the redistribution, or scattering, of their energy in wavevector space [1]. In an effort to quantify this scattering, we have developed theoretical models based on two key assumptions: (i) weak flow, in the sense that the typical flow speed U is much smaller than the typical IGW group speed c, that is, $U \ll c$; and (ii) random flows, represented by homogeneous, stationary random functions with prescribed statistics. In addition, the flows have been assumed in geostrophic balance, so that the statistics of a single random streamfunction need to be prescribed; for simplicity the streamfunction is taken to be isotropic in the horizontal. Established methods for waves in random media then lead to a kinetic equation for $a(\mathbf{x}, \mathbf{k}, t)$, the density of IGW action in the $(\mathbf{x}, \mathbf{k})$ phase space. This equation takes the standard form

$$\partial_t a + \nabla_{\mathbf{k}}\omega \cdot \nabla_{\mathbf{x}} a - \nabla_{\mathbf{x}}\omega \cdot \nabla_{\mathbf{k}} a = \int \sigma(\mathbf{k}, \mathbf{k}') a(\mathbf{x}, \mathbf{k}', t)\, \mathrm{d}\mathbf{k}' - \Sigma(\mathbf{k}) a(\mathbf{x}, \mathbf{k}, t), \tag{1}$$

where $\omega(\mathbf{k})$ is the intrinsic frequency of IGWs, and $\Sigma(\mathbf{k}) = \int \sigma(\mathbf{k}, \mathbf{k}')\, \mathrm{d}\mathbf{k}'$. The scattering cross-section $\sigma(\mathbf{k}, \mathbf{k}')$ is given explictly in [2] under the assumption that the geostrophic flow is time independent. Its salient properties are that it is proportional to the geostrophic-flow energy spectrum and to $\delta(\omega(\mathbf{k}) - \omega(\mathbf{k}'))$. The latter property implies that energy is scattered only between IGWs with the same frequency; that is, energy transfers are restricted to a constant-frequency surface in wavevector space, a cone for IGWs. This is a simple consequence of the wave linearity and the time independence of the geostrophic flow.

A convenient approximation to (1) can be obtained in the WKB limit of IGWs short compared with typical geostrophic-flow scales. The scattering integral then reduces to a simple diffusion in wavevector space, leading to

$$\partial_t a + \nabla_{\mathbf{k}}\omega \cdot \nabla_{\mathbf{x}} a - \nabla_{\mathbf{x}}\omega \cdot \nabla_{\mathbf{k}} a = \nabla_{\mathbf{k}} \cdot (\mathsf{D} \nabla_{\mathbf{k}} a)\,, \tag{2}$$

with a $\mathbf{k}$-dependent diffusivity tensor D that can be deduced from $\sigma(\mathbf{k}, \mathbf{k}')$ or obtained directly [3, 4]. The time independence of the flow and consequent restriction of the scattering to the constant-frequency cone is reflected in the degeneracy of the diffusivity, which satisfies $\mathsf{D} \cdot \nabla_{\mathbf{k}}\omega = 0$. A remarkable feature of (2) is that, for a spatially homogeneous wave forcing and a three-dimensional geostrophic flow, it predicts stationary action and energy spectra obeying the power law $|\mathbf{k}|^{-2}$, reminiscent of atmospheric and oceanic observations [3].

The assumption of time independence of the geostrophic flow can be relaxed using a perturbative approach based on the smallness of the ratio ε of the IGW period to the geostrophic-flow time scale. In the diffusive approximation (2), this leads to a correction $\varepsilon^2 \mathsf{D}'$ to the diffusivity, which includes a component normal to the constant-frequency cone, $\mathsf{D}' \cdot \nabla_{\mathbf{k}}\omega \neq 0$. An asymptotic analysis of the diffusion

equation shows that this component leads to a smooth distribution of IGW energy that remains localised for all times within an $O(\varepsilon)$ boundary layer around the cone corresponding to the forcing frequency [5]. This is in contrast with results obtained in two-dimensional models such as the rotating shallow-water system [6].

We conclude with two remarks. First, while the theory leading to (1)–(2) has been developed for a turbulent flow with homogeneous statistics, it can be extended straightforwardly to include a deterministic, large-scale flow (to represent, e.g., atmospheric jets) by adding the corresponding Doppler-shift contribution to the intrinsic frequency, thus replacing ω by $\omega + \mathbf{k} \cdot \mathbf{U}$. Second, the right-hand sides of (1)–(2) could be used to parameterise the effect of an unresolved flow (whose energy spectrum is known, say from observations). With this in mind, it is interesting that these right-hand sides can be identified as the generators of two stochastic processes – Markov jump process and diffusion, respectively – and hence have a natural stochastic parameterisation.

References

[1] Young W. R. 2021 Inertia-gravity waves and geostrophic turbulence. *J. Fluid Mech.* **920**, F1.

[2] Savva M. A. C., Kafiabad H. A. & Vanneste J. 2021 Inertia-gravity-wave scattering by three-dimensional geostrophic turbulence, *J. Fluid Mech.* **916**, A6.

[3] Kafiabad H. A., Savva M. A. C. & Vanneste J. 2019 Diffusion of inertia-gravity waves by geostrophic turbulence, *J. Fluid Mech.* **869**, R7.

[4] McComas C. H. & Bretherton F. P. 1977 Resonant interaction of oceanic internal waves. *J. Geophys. Res.* **82**, 1397–1412.

[5] Cox M. R., Kafiabad H. A. & Vanneste J. 2022 Inertia-gravity-wave diffusion by geostrophic turbulence: the impact of flow time dependence, submitted, arXiv:2207.09386.

[6] Dong, W., Bühler O. & Smith K. S. 2020 Frequency diffusion of waves by unsteady flows. *J. Fluid Mech.* **905**, R3.

Uncertain turbulent fluxes in the atmospheric boundary layer: a stochastic data-model fusion approach

Nikki Vercauteren

(joint work with Vyacheslav Boyko, Sebastian Krumscheid)

Limited computer resources lead to a simplified representation of unresolved small-scale processes in weather and climate models, through parameterisation schemes. Among the parameterised processes, turbulent fluxes exert a critical impact on the exchange of heat, water and carbon between the land and the atmosphere. Turbulence theory relies on Monin-Obukhov Similarity theory (MOST), which was developed for homogeneous and flat terrain, with stationary conditions. The theory fails in unsteady flow contexts or with heterogeneous landscapes, but no alternative, viable theory is available. This is not only a source of error in forecasts or climate scenarios, but also a source of model uncertainty which should be characterised and considered when using weather and climate models.

This work seeks to generalise MOST by enabling an explicit treatment of uncertainty of the fluxes to be modelled, thereby representing the model uncertainty

arising from the incomplete representation of our unsteady atmosphere. This is particularly relevant in cold environments or at nighttime, where the atmospheric boundary layer is stably stratified. Turbulence then coexists with non-turbulent motions from the so-called grey zone between the largest turbulent eddies and smallest mesoscale motions, traditionally specified to be 2km horizontal scale. These non-turbulent motions can include density currents, wave-like motions or two-dimensional modes and represent a non-stationary forcing of turbulence. The non-stationary forcing can occur on scales overlapping with the turbulent scales, thereby preventing the possibility of reaching a quasi-equilibrium of turbulence assumed in classical MOST. Hence a generalisation of MOST should relax the traditional assumption of stationarity and instead account for mixing and transport due to non-stationary, unresolved sub-mesoscale motions, but also for departures from statistical equilibrium of the turbulence itself. Both aspects are intertwined by nonlinear feedback processes, leading to additional uncertainty in the resulting unresolved mixing that needs to be parametrised in numerical weather prediction models.

The generalisation of MOST is inspired by the emerging use of stochastic parameterisations in weather forecasting, as those provide an attractive solution to include the model uncertainty when representing unresolved processes. Stochastic parameterisations have had a tremendous impact on probabilistic weather prediction, the most important one being to have increased reliability and skill of forecasts. Stochastic parameterisations represent atmospheric processes as a combination of a predictable deterministic and an unpredictable stochastic component. One key aspect in the development of stochastic parameterisations is to include uncertainty in a physically meaningful way. For this, the functional form of the parametrisation schemes and their parameters, which represent small-scale effects and are generally unknown, must be uncovered. With appropriate data-driven stochastic modelling strategies, observational data can be optimally exploited to uncover scaling of the parameters of a stochastic model with resolved-scale dynamics.

Such a data-driven stochastic modelling strategy was introduced in [1] to estimate the parametrisation of unresolved degrees of freedom in a complex system. Based on numerical experiments, [1] demonstrated that the method could uncover scaling of the SDE model parameters with slow modulating variables, based solely on observed timeseries of the process to be parameterised. The approach therefore provides an ideal framework to derive stochastic subgrid-scale models which are modulated by mean-flow, resolved variables. Using turbulence measurements from a field site, this method is hence used to derive a stochastic generalisation of MOST. A critical choice in the application of the model-fitting method is that of the variable to be modelled as a stochastic process. In MOST, turbulent fluxes are related to the mean gradients at the surface through the use of a function of a dimensionless parameter that encodes the combined influence of the static stability of the atmosphere and of shear forces. The so-called universal functions are determined using experimental data and provide an adjustment of the turbulence

mixing length according to the atmospheric stability. This stability correction modelled empirically in MOST is hence selected as the most natural candidate for a stochastic extension to MOST.

When fitting the stochastic stability correction based on data collected at one field site under conditions of stable stratification, a stochastic differential equation parameterisation is obtained in which the parameters scale with the classical dimensionless parameter used in MOST. The resulting stochastic stability equation adequately captures the invariant density of the observations and hence quantifies the uncertainty of the stability correction variables. The statistics of the stability correction are non-Gaussian, reflecting the intermittent behaviour of turbulent mixing. The stochastic parameterisation extends conventional models and enables the representation of unsteady, intermittent fluxes. It could help overcome some of the limitations of weather and climate models to represent mixing in the stable boundary layer.

A broader validity of the stochastic equation is questionable and should be explored in other field experiments. The important questions to investigate are: How general is the functional form of the stochastic model? How much of the uncertainty of MOST, here attributed to the impact of sub-mesoscale motions and intermittency of turbulence, could actually be systematically related to local heterogeneity of the land surface? These aspects would be critical for implementation of the approach in numerical weather forecasting.

References

[1] V. Boyko, S. Krumscheid and N. Vercauteren *Statistical learning of non-linear stochastic differential equations from non-stationary time-series using variational clustering*, Multiscale Modeling & Simulation, in press (2022).

MS-GWaM – A three dimensional transient parametrization for internal gravity waves in atmospheric models

Georg S. Voelker

(joint work with Young-Ha Kim, Gergely Bölöni, Günther Zängl, Ulrich Achatz)

Subgrid-scale internal gravity waves (IGWs) are important distributors of energy and momentum in a stratified atmosphere. While they are mostly excited at lower altitudes their effects are most important between the upper troposphere to the mesopause at altitudes ∼85km [3]. While propagating—both in the vertical and the horizontal—nonlinear IGWs can exert a wave drag on the mean winds, interact with the mean potential temperature, and mix atmospheric tracers such as aerosols or greenhouse gases [1, 2, 3, 6, 8, 10, 11].

In state-of-the art weather prediction models IGWs are typically parametrized neglecting both the horizontal wave propagation (single-column assumption) and the transient wave behavior including wave-mean-flow interactions and time dependent wave generation (steady-state assumption) [4]. The potential importance

of the horizontal wave propagation and wave transience has, however, been shown in various theoretical, numerical and experimental studies [6, 9, 10, 11].

Here we present recent advances of the use of the transient Multi Scale Gravity Wave Model (MS-GWaM) in the upper atmosphere model UA-ICON. The underlying wave theory is based on a multi scale WKBJ analysis of the compressible atmosphere and solved numerically through a parallelized Lagrangian ray-tracing scheme [7, 8]. To avoid caustics the wave action of each spectral component, $\mathcal{A}_\alpha$, is expanded into a phase space wave action density, $\mathcal{N}$, to rewrite the wave action conservation in the absence of dissipation as follows [7]

$$0 = \partial_T \mathcal{N} + \mathbf{c}_g \cdot \nabla_{\mathbf{X}} \mathcal{N} + \dot{\mathbf{k}} \cdot \nabla_{\mathbf{k}} \mathcal{N},$$

where $\mathbf{c}_g$ and $\dot{\mathbf{k}}$ are the group velocity and the rate of change of the wave vector along the path of propagation, respectively. It is worth mentioning that the phase space volume is conserved under such a transformation. This formulation thus allows to solve the well known gravity wave ray equations for a set of spectral components which may coexist at the same location. Based on this we construct a parametrization including various non-orographic wave sources, three dimensional transient propagation, direct wave-mean-flow interactions and a Lindzen type wave saturation [2]. Nonlinear triad interactions are neglected at this point.

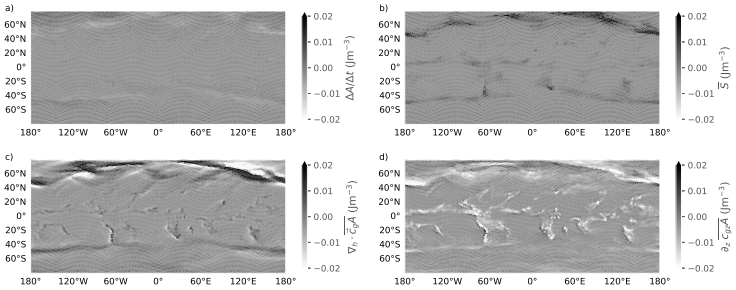

FIGURE 1. Components of the 3-dimensional, time averaged wave action conservation for a 1 week period. The change in wave action (a) is small relative to the horizontal (c) and vertical (d) wave action divergence. The wave action flux divergence (c + d) therefore approximately balances with the wave dissipation (b). Note that (c) is set to zero in the 1-dimensional case so that (b) and (d) approximately balance.

Simulation results show a satisfactory reproduction of the observed mean wind and potential temperature climatology while revealing new insight into the details of the role of internal gravity waves in the atmosphere. In particular, probability density functions of wave momentum fluxes exhibit the typical observed long tails (i.e. wave intermittency) which cannot be reproduced with steady-state

parametrizations beyond the intermittency of the wave sources. Moreover, the three dimensional distribution of wave action fluxes differ greatly when relaxing the single-column assumption. In particular, we find that the horizontal part of the wave action flux divergence is of the same order of magnitude relative to the vertical part and thus plays an important role in shaping the global wave action and thus wave energy balance (Fig. 1).

Albeit exhibiting promising new insight and a more physical wave behavior compared to 1-dimensional or steady-state schemes it must be noted that the current stage of MS-GWaM still depends on various simplifications. In particular the majority of generation processes are summarized in a single background source using the scheme of Orr et al. [5] and orographic waves are not included. It is planned to mend that shortcoming and explicitly include orographic waves as well as various wave sources such as gravity waves generated by fronts and jet systems. Having a broader perspective in mind it is envisioned to build a robust tool for the investigation of both local and large scale internal gravity effects in the atmosphere.

References

[1] Grimshaw, R., *Nonlinear internal gravity waves in a rotating fluid*, Journal of Fluid Mechanics **71(3)** (1975), 497–512.

[2] Lindzen, R. S., *Turbulence and stress owing to gravity wave and tidal breakdown*, Journal of Geophysical Research **86(C10)** (1981), 9707–9714.

[3] Becker, E. and Schmitz, G., *Climatological effects of orography and land-sea heating contrasts on the gravity wave-driven circulation of the mesosphere*, Journal of the Atmospheric Sciences **60(1)** (2003), 103–118.

[4] Young-Joon Kim, Stephen D. Eckermann, Hye-Yeong Chun, *An overview of the past, present and future of gravity-wave drag parametrization for numerical climate and weather prediction models*, Atmosphere-Ocean **41:1** (2003), 65–98

[5] Orr, A., Bechtold, P., Scinocca, J., Ern, M., and Janiskova, M., *Improved middle atmosphere climate and forecasts in the ECMWF model through a nonorographic gravity wave drag parameterization*, Journal of Climate **23(22)** (2010), 5905–5926.

[6] Senf, F. and Achatz, U., *On the impact of middle-atmosphere thermal tides on the propagation and dissipation of gravity waves*, Journal of Geophysical Research Atmospheres **116(24)** (2011)

[7] Muraschko, J., Fruman, M. D., Achatz, U., Hickel, S., and Toledo, Y., *On the application of Wentzel-Kramer-Brillouin theory for the simulation of the weakly nonlinear dynamics of gravity waves*, Quarterly Journal of the Royal Meteorological Society **141(688)** (2015), 676–697.

[8] Achatz, U., Ribstein, B., Senf, F., and Klein, R., *The interaction between synoptic-scale balanced flow and a finite-amplitude mesoscale wave field throughout all atmospheric layers: weak and moderately strong stratification*, Quarterly Journal of the Royal Meteorological Society **143(702)** (2017), 342–361

[9] Wei, J., Bölöni, G., and Achatz, U., *Efficient modeling of the interaction of mesoscale gravity waves with unbalanced large-scale flows: Pseudomomentum-Flux Convergence versus Direct Approach*, Journal of the Atmospheric Sciences **76(9)** (2019), 2715–2738

[10] Bölöni, G., Kim, Y.-H., Borchert, S., and Achatz, U., *Towards transient subgrid-scale gravity wave representation in atmospheric models. Part I: Propagation model including direct wave-mean-flow interactions*, Journal of the Atmospheric Sciences **78(4)** (2021), 1317–1338

[11] Kim, Y.-H., Bölöni, G., Borchert, S., Chun, H.-Y., and Achatz, U., *Toward transient subgrid-scale gravity wave representation in atmospheric models. part ii: Wave intermittency simulated with convective sources*, Journal of the Atmospheric Sciences **78(4)** (2021), 1339–1357.

Instability and turbulent mixing in wind-driven shear layers

Gregory L. Wagner
(joint work with Nick Pizzo, Luc Lenain, Fabrice Veron)

Approximate parameterizations for turbulent fluxes across the ocean surface boundary layer are core components of ocean and climate models. Boundary layer turbulence parameterizations are typically calibrated not to observations, but to synthetic data generated by large eddy simulations of ocean surface boundary layer turbulence. The accuracy of climate predictions thus hinges on the fidelity of these large eddy simulations, which in turn depend worryingly on numerous approximations that remain largely uncharacterized.

One of the approximations invoked by simulations of ocean surface boundary layer turbulence is to account for wave-turbulence interactions with the Craik-Leibovich equation [2, 3, 6, 4],

$$\partial_t \mathbf{u}^L + \left(\mathbf{u}^L \cdot \nabla\right) \mathbf{u}^L + \left(\nabla \times \mathbf{u}^S\right) \times \mathbf{u}^L + \nabla \bar{p} = \nu \triangle \mathbf{u}^L - \nu \triangle \mathbf{u}^S + \partial_t \mathbf{u}^S \,, \tag{1}$$

where $\mathbf{u}^L$ is the Lagrangian-mean velocity field, $\mathbf{u}^S$ is the surface wave Stokes drift, $\bar{p}$ is the Eulerian-mean kinematic pressure, and ν is the kinematic viscosity. Equation 1 describes the catalytic, organizing effects of surface waves on boundary layer turbulent motions through the "effective background vorticity" term $\left(\nabla \times \mathbf{u}^S\right) \times \mathbf{u}^L$ [7, 4, 1]. However, equation 1 does not describe the effects of wave breaking and fast wave-turbulence interaction.

We provide a preliminary validation of the Craik-Lebovich equations using wave-averaged simulations of 1 that reproduce deceptively simple laboratory experiments performed by Veron and Melville (2001) [8]: wind rising over calm, unstratified water. In these experiments, the developing wind drives the growth of a surface wave field and accelerates a sheared current until it transitions to turbulence by "Langmuir instability" and then deepens through turbulent mixing.

Our primary result is that simulations of the Craik-Leibovich equation 1 reproduce basic aspects of instability and subsequent turbulent shear layer deepening observed in the laboratory experiments, despite using a horizontally-periodic domain and idealizing the surface wave as steady and monochromatic. This result is illustrated by figure 1, which shows time series of surface velocity statistics and visualizations of the streamwise velocity and a synthetic surface concentrated tracer. In figure 1, the development of the primary instability, is marked by the divergence of the mean, minimum, and maximum streamwise surface velocity around $t = 17$ seconds. The growth of the primary instability is quickly interrupted around $t = 18$ seconds by a secondary instability that causes the maximum surface velocity to decrease. The simulations reproduce the evolution of both the primary and secondary instability. In the final phase of the experiment (where laboratory data is uninformative), turbulence mixes momentum and an initially surface concentrated tracer downwards.

We further contrast simulations with and without wave effects to show that (i) the presence of surface waves is required to trigger instability at laboratory

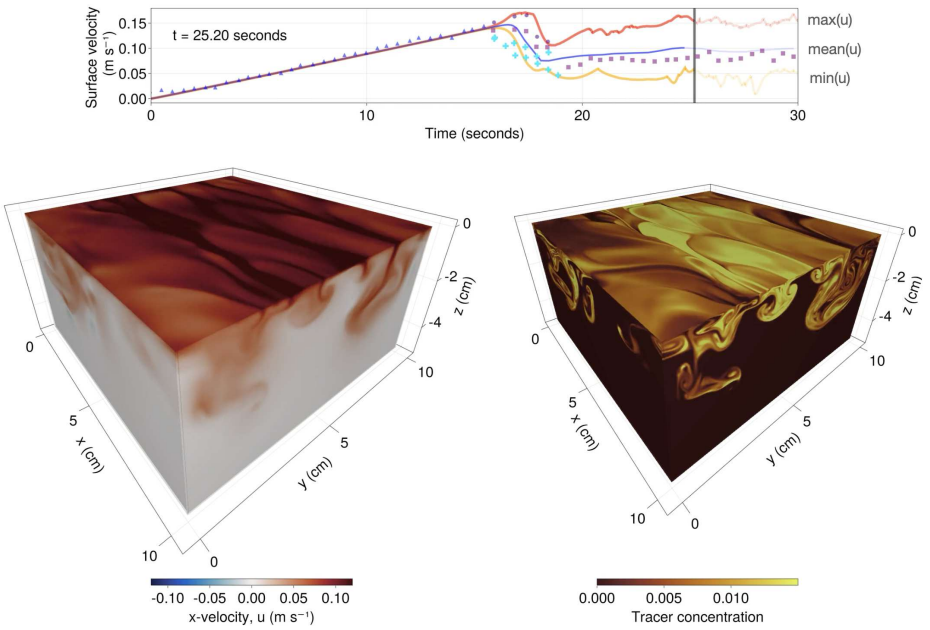

FIGURE 1. Data from simulations of laboratory experiments by Veron and Melville (2001) [8] on boundary layers driven by increasing winds oriented in the x-direction. (Top) time series of surface velocity statistics showing that the simulated surface velocity field statistics (lines) closely track the laboratory data (symbols, see also figure 9 from [8]). (Bottom left) three-dimensional visualization of the streamwise velocity field at $t = 25.2$ seconds. (Bottom right) visualization of an initially surface-concentrated tracer.

Reynolds numbers, (ii) the primary instability is sensitive to the nonlinear amplitude of the surface waves, but not to their wavenumber, and (iii) after instability, the presence of surface waves accelerates the turbulent deepening of the shear layer.

REFERENCES

[1] Wagner, Gregory L and Chini, Gregory P and Ramadhan, Ali and Gallet, Basile and Ferrari, Raffaele, *Near-inertial waves and turbulence driven by the growth of swell*, Journal of Physical Oceanography, **51**:5 (2021), 1337–1351

[2] Craik, Alex D. D. and Leibovich, Sidney, *A rational model for Langmuir circulations*, Journal of Fluid Mechanics, **73**:3 (1976), 401–426

[3] Huang, N. E., *On surface drift currents in the ocean*, Journal of Fluid Mechanics, **91**:1 (1979), 191–208

[4] Sullivan, Peter P and McWilliams, James C, *Dynamics of winds and currents coupled to surface waves*, Annual Review of Fluid Mechanics, **42** (2010), 19–42
[5] Melville, W Kendall, *The role of surface-wave breaking in air-sea interaction*, Annual review of fluid mechanics, **28**:1 (1996), 279–321
[6] Suzuki, Nobuhiro and Fox-Kemper, Baylor, *Understanding Stokes forces in the wave-averaged equations*, Journal of Geophysical Research: Oceans, **121**:5 (2016), 3579–3596
[7] McWilliams, James C and Sullivan, Peter P and Moeng, Chin-Hoh, *Langmuir turbulence in the ocean*, Journal of Fluid Mechanics, **334** (1997), 1–30
[8] Veron, Fabrice and Melville, W Kendall, *Experiments on the stability and transition of wind-driven water surfaces*, Journal of Fluid Mechanics, **446** (2001), 25–65

A deep learning approach to extract surface internal tidal signals scattered by geostrophic turbulence

Han Wang
(joint work with Nicolas Grisouard, Hesam Salehipour, Alice Nuz, Michael Poon, Aurélien L. Ponte, Brian Arbic)

Internal tides (ITs) are inertia-gravity waves generated by oceanic barotropic tides (large-scale, vertically uniform tidal currents) flowing over topography, important to oceanographers due to their roles in problems such as deep/upper ocean mixing. Conventionally, for altimetric observations of Sea Surface Height (SSH) data, ITs have been extracted by harmonically fitting over observed time sequences. However, in presence of strong time-dependent phase shifts induced by interactions with mean flows or changes in stratifications, harmonic fits do not work well for data with coarse temporal sampling. This problem would be exacerbated in the upcoming Surface Water Ocean Topography (SWOT) satellite mission due to the finer spatial scales to be resolved.

However, SWOT's wide swaths will unprecedentedly produce SSH snapshots that are spatially two-dimensional, which allows the community to treat tidal extraction as an operation on two-dimensional images. Here, we regard tidal extraction purely as an image translation problem. We design and train a conditional Generative Adversarial Network(cGAN), which, given a snapshot of raw SSH, generates a snapshot of the embedded tidal component. In the talk, we introduce a recent work ([1]), where we train and test the cGAN on a set of idealized numerical eddying simulation. No temporal information or physical knowledge is required for the cGAN to work in this experiment. We test the cGAN on data whose dynamical regimes are different from the data provided during training. Despite the diversity and complexity of data, it accurately extracts tidal components in most individual snapshots considered and reproduces physically meaningful statistical properties. Predictably, the cGAN's performance decreases with the intensity of the turbulent flow.

Our cGAN is still steps away from being practically applicable for real altimetric data. As a brief discussion of an ongoing work, we present some preliminary results on the performance of cGAN on outputs from HYCOM, a more realistic oceanic model ([2]), where the cGAN conduct a meaningful temporal frequency filterings

in selected spatial regions, despite that no temporal information is added during training/testing. Other possible improvements include incorporating physics-informed forcings, testing the performance in presence of measurement noise, and combinations with other recent IT extraction attempts.

Broadly speaking, the project, just as most deep-learning applications, is motivated from a utilitarian perspective: we don't necessarily understand why the cGAN works so well, and we use it because it outperforms classical IT extraction methods, at least in our idealized data sets. As far as we know, this is the first time an image-based cGAN is applied in atmospheric/oceanic fluid dynamics, and could be applied in other problems too. To those who might be uncomfortable with black boxes, we argue that it is at least a tool to indicate the solvability of a problem: IT extraction is shown to be possible purely based on spatial information, and with this information, perhaps one could find a fully interpretable method to achieve the same goal.

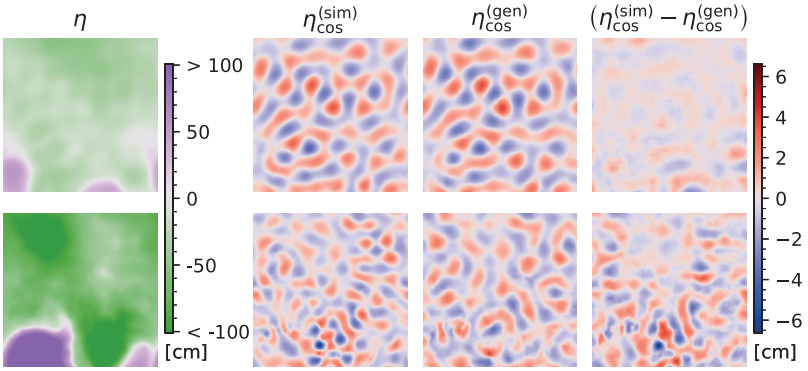

FIGURE 1. Tidal reconstruction example during testing stage; upper and lower row correspond to the best and worst examples respectively.

REFERENCES

[1] Wang, Han and Grisouard, Nicolas and Salehipour, Hesam and Nuz, Alice and Poon, Michael and Ponte, Aurelien L.S., *A deep learning approach to extract internal tides scattered by geostrophic turbulence*, Geophysical Research Letters **49/11** (2022), e2022GL099400.

[2] Arbic, Brian K and Richman, James G and Shriver, Jay F and Timko, Patrick G and Metzger, E Joseph and Wallcraft, Alan J, *Global modeling of internal tides: Within an eddying ocean general circulation model*, Oceanography **25/2** (2012), 20–29.

Reporter: Oliver Bühler

Participants

Prof. Dr. Ulrich Achatz
FB Geowissenschaften/Geographie
Institut für Atmosphäre und Umwelt
Johann Wolfgang Goethe Universität
Altenhöferallee 1
60438 Frankfurt am Main
GERMANY

Dr. Triantaphyllos Akylas
Department of Mechanical Engineering
MIT
Cambridge, MA 02139
UNITED STATES

Dr. Roy Barkan
Department of Geophysics
Tel Aviv University
P.O.Box 39040
Ramat Aviv, Tel Aviv 69978
ISRAEL

Ashley Barnes
Centre for Mathematics & its Application
Australian National University
Canberra ACT 0200
AUSTRALIA

Prof. Dr. Oliver Bühler
Center for Atmosphere Ocean Science
Courant Institute of Mathematical Sciences
New York University
251, Mercer Street
New York, NY 10012-1110
UNITED STATES

Dr. Hans Burchard
Leibniz Institute
for Baltic Sea Research
Seestr. 15
18119 Warnemünde
GERMANY

Prof. Dr. Jörn Callies
Caltech
1200 E. California Blvd.
P.O. Box MC 131-24
Pasadena CA 91125
UNITED STATES

Prof. Dr. Paola Cessi
Scripps Institution of Oceanography
University of California, San Diego
9500 Gilman Drive
La Jolla CA, 92093-0213
UNITED STATES

Dr. Ray Chew
Institute for Atmospheric and Environmental Sciences
Goethe-Universität Frankfurt
Altenhöferallee 1
60438 Frankfurt am Main
GERMANY

Prof. Dr. Colin Cotter
Department of Mathematics
Imperial College London
South Kensington Campus
London SW7 2AZ
UNITED KINGDOM

Dr. Bruno Deremble
Geosciences Institute
Université de Grenoble
70 Rue de la physique
38402 Saint-Martin-d'Hères Cedex
FRANCE

Prof. Dr. Stamen Dolaptchiev
Johann Wolfgang Goethe Universität
Fachbereich
Geowissenschaften/Geographie
Altenhöferallee 1
60438 Frankfurt am Main
GERMANY

Prof. Dr. Bérengère Dubrulle
SPHYNX SPEC
CEA Orme des Merisiers
P.O. Box 774
91191 Gif-sur-Yvette
FRANCE

Prof. Dr. Carsten Eden
Institut für Meereskunde der
Universität Hamburg
Bundesstr. 53
20146 Hamburg
GERMANY

Dr. Raffaele Ferrari
Department of Earth, Atmospheric
and Planetary Sciences
Massachusetts Institute of Technology
77 Massachusetts Avenue
54-1620 Cambridge MA 02139
UNITED STATES

Dr. Mara Freilich
Scripps Institution of Oceanography
University of California, San Diego
9500 Gilman Drive
La Jolla, CA 92093-0112
UNITED STATES

Prof. Dr. Edwin Gerber
Center for Atmosphere Ocean Science
Courant Institute of Math. Sc.
New York University
251 Mercer Street
New York, NY 10012-1110
UNITED STATES

Prof. Dr. Nicolas Grisouard
Department of Physics
University of Toronto
60 St. George Street
Toronto ON M5S 1A7
CANADA

Prof. Dr. Pedram Hassanzadeh
6100 Main Street, Houston TX 77005
Rice University
Houston TX 77005-1892
UNITED STATES

Dr. Sylvain Joubaud
ENS de Lyon
Laboratoire de Physique
46, Allee d'Italie
69007 Lyon Cedex
FRANCE

Dr. Hossein Kafiabad
School of Mathematics
University of Edinburgh
James Clerk Maxwell Bldg.
King's Buildings, Mayfield Road
Edinburgh EH9 3FD
UNITED KINGDOM

Prof. Dr. Rupert Klein
Fachbereich Mathematik und Informatik
Freie Universität Berlin
Arnimallee 6
14195 Berlin
GERMANY

Dr. Laura Köhler
Max Planck Institute for Meteorology
Bundesstraße 53
20146 Hamburg
GERMANY

Dr. Stephane Le Dizes
Institut de Recherche sur les
Phénomènes Hors Equilibre (IRPHE),
CNRS, Aix Marseille Université
49 rue Frédéric Joliot-Curie
13013 Marseille
FRANCE

Dr. Pascale Lelong
Northwest Research Associates
4118 148th Ave NE
Redmond WA 98052-5164
UNITED STATES

Dr. Stefan Llewellyn Smith
MAE and SIO
University of California, San Diego
9500 Gilman Drive
La Jolla, CA 92093-0411
UNITED STATES

Dr. Marvin Lorenz
Leibniz-Institut für Ostseeforschung
Seestraße 15
18119 Rostock
GERMANY

Dr. Francois Lott
Laboratoire de Meteorologie Dynamique
Ecole Normale Superieure
24, rue Lhomond
75231 Paris Cedex 05
FRANCE

Prof. Dr. Leo Maas
Physics, Institute for Marine and
Atmospheric Research Utrecht (IMAU)
Universiteit Utrecht
Princetonplein 5
3584 CC Utrecht
NETHERLANDS

Dr. Gökce Tuba Masur
Goethe Universität Frankfurt
Institut für Atmosphäre und Umwelt
Altenhöferallee 1
60438 Frankfurt am Main
GERMANY

Dr. Claire Menesguen
Laboratoire d'Océanographie Physique
et Spatiale
Ifremer
ZI de la Pointe du Diable
29280 Plouzane
FRANCE

Prof. Dr. Sergey Nazarenko
Institute de Physique de Nice, C.N.R.S.,
Université de la Côte D'Azur
Parc Valrose
06108 Nice Cedex 2
FRANCE

Nicolas Perez
Laboratoire de Physique
École Normale Superieure de Lyon
46, Allee d'Italie
69364 Lyon Cedex 07
FRANCE

Dr. Aurelien Podglajen
Ecole Polytechnique
91128 Palaiseau Cedex 16
FRANCE

Dr. Inna Polichtchouk
ECMWF
Shinfield Road
Reading RG2 9AX
UNITED KINGDOM

Dr. Costanza Rodda
South Kensington campus
Skempton building
Imperial college London
Department of civil and environmental
engineering
SW7 2AZ London
UNITED KINGDOM

Dr. Callum Shakespeare
Research School of Earth Sciences
Australian National University
142 Mills Rd
2601 Acton 2601
AUSTRALIA

Dr. Aditi Sheshadri
Stanford University
Earth system science
473 Via Ortega
Palo Alto CA 94305
UNITED STATES

Prof. Victor Shrira
School of Computing and Mathematics
University of Keele
MacKay building. Office 2.10
Keele
ST5 5BG Keele, Newcastle, Staffs, ST5 5BG
UNITED KINGDOM

Prof. Dr. Shafer Smith
Courant Institute of Mathematical Sciences
New York University
251, Mercer Street
New York, NY 10012-1110
UNITED STATES

Dr. Joel Sommeria
Laboratoire des Ècoulements Géophysiques et Industriels (LEGI)
1209 Rue da la Piscine
38610 Grenoble
FRANCE

Prof. Dr. Peter Spichtinger
Institute for Atmospheric Physics (IPA)
Johannes Gutenberg University Mainz
Johann-Joachim-Becher-Weg 21
55128 Mainz
GERMANY

Prof. Dr. Chantal Staquet
Laboratoire LEGI
Domaine Universitaire
CS 40700
38058 Grenoble Cedex 9
FRANCE

Dr. Ivana Stiperski
Department of Atmospheric and Cryospheric Sciences
University of Innsbruck
Innrain 52
6020 Innsbruck
AUSTRIA

Dr. Bruce Sutherland
Department of Physics, CCIS 4-181
University of Alberta
Edmonton T6G 2E1
CANADA

Prof. Dr. Esteban G. Tabak
Courant Institute of Mathematical Sciences
New York University
251, Mercer Street
New York, NY 10012-1110
UNITED STATES

Dr. Jim Thomas
International Centre for Theoretical Sciences and
Centre for Applicable Mathematics
Tata Institute of Fundamental Research
Bangalore, Bengaluru
INDIA

Prof. Dr. Geoffrey K. Vallis
Department of Mathematics
University of Exeter
North Park Road
Exeter EX4 4QE
UNITED KINGDOM

Dr. Jacques Vanneste
School of Mathematics
University of Edinburgh
James Clerk Maxwell Bldg.
King's Buildings, Peter G Tait Road
Edinburgh EH9 3FD
UNITED KINGDOM

Dr. Nikki Vercauteren
Department of Geosciences, Section for Meteorology and Oceanography,
University of Oslo
0371 Oslo
NORWAY

Dr. Bruno Voisin
Laboratoire des Écoulements Géophysiques et Industriels (LEGI)
1209 Rue de la Piscine
P.O. Box CS 40700
38058 Grenoble Cedex 9
FRANCE

Dr. Georg Sebastian Völker
Goethe Universität Frankfurt
Institut für Atmosphäre und Umwelt
Altenhöferallee 1
60438 Frankfurt am Main
GERMANY

Gregory Wagner
Department of Earth, Atmospheric, and Planetart Sciences
Massachusetts Institute of Technology
77 Massachusetts Ave
02139 Cambridge 02139
UNITED STATES

Dr. Han Wang
School of Mathematics
University of Edinburgh
James Clerk Maxwell Bldg.
Office 4622
Peter Guthrie Tait Road
Edinburgh EH9 3FD
UNITED KINGDOM

Prof. Dr. Beth Wingate
Department of Mathematics and Statistics
University of Exeter
Harrison Building
North Park Road
Exeter EX4 4QF
UNITED KINGDOM

Dr. Jin-Han Xie
Department of Mechanics and Engineering Science
Peking University
Beijing 100871
CHINA

Prof. Dr. William R. Young
Scripps Institution for Oceanography
University of California, San Diego
9500 Gilman Drive
La Jolla CA 92093-0213
UNITED STATES